NUMERICAL METHOD DEVELOPMENT FOR COOLING OF END WINDINGS OF AN ELECTRIC MOTOR

A THESIS SUBMITTED IN PARTIAL FULFILLMENT OF
REQUIREMENTS FOR THE DEGREE OF

MASTER OF ENGINEERING

IN

THERMAL ENGINEERING

BY

ANUBHAV

REGISTRATION NO: 802183001

UNDER THE SUPERVISION OF

Dr. Vikrant Khullar (Associate Professor)
Department of Mechanical Engineering,
Thapar Institute of Engineering & Technology, Patiala

Mr. Nagesh Biradar
(Senior Engineer)
MS/ENF1, Bosch Global Software Technologies Pvt Ltd. Bangalore

Dr. Rajesh Kumar Shukla (Asst. Professor)
Department of Mechanical Engineering,
Thapar Institute of Engineering & Technology, Patiala

THAPAR INSTITUTE
OF ENGINEERING & TECHNOLOGY
(Deemed to be University)

MECHANICAL ENGINEERING DEPARTMENT

THAPAR INSTITUTE OF ENGINEERING & TECHNOLOGY, PATIALA

CERTIFICATE

I hereby declare that the dissertation entitled **"Numerical Method Development for Cooling of End Windings of an Electric Motor"** is an authentic record of my work carried out in my internship at Bosch Global Software Technology (BGSW) and as a requirement for the award of the degree of Master of Engineering in Thermal Engineering at Thapar Institute of Engineering and Technology, Patiala under the support and guidance of Dr. Vikrant Khullar (Associate Professor) and Dr. Rajesh Kumar Shukla (Assistant Professor), Mechanical Engineering Department.

I hereby declare that if I violate the intellectual property rights or copyrights found at any stage, I will be solely responsible for the same. And no part of the matter embodied in this report has been submitted to any other university or institute for the award of any degree.

Anubhav
M.E (Thermal Engineering)
Roll no.: 802183001

It is to be certified that the above statement is correct to the best of my knowledge and belief.

Dr. Vikrant Khullar
Associate Professor
Mechanical Engineering Department

Dr. Rajesh Kumar Shukla
Assistant Professor
Mechanical Engineering Department

INTERNSHIP CERTIFICATE

BOSCH
Invented for life

Bosch Global Software Technologies Pvt. Ltd.

CERTIFICATE

This is to certify that **Mr. Anubhav**, Roll No. **802183001** a Bonafide Masters (Thermal) student of Thapar Institute of Engineering and Technology, Patiala, has successfully completed his internship on topic "Numerical Method Development for cooling End windings of an Electric motor" at Bosch Global Software Technologies Pvt. Ltd., Bangalore from 20th June 2022 to 28th April 2023.

pki, BOSCH, APAC, N, A, Nagesh.Biradar Digitally signed by pki, BOSCH, APAC, N, A, Nagesh.Biradar Date: 2023.05.05 09:23:24 +05'30'	pki, BOSCH, APAC, R, A, Ramakrishna.Derisala Digitally signed by pki, BOSCH, APAC, R, A, Ramakrishna.Derisala Date: 2023.05.05 09:26:12 +05'30'
Mr. Nagesh Biradar	**Mr. Derisala Ramakrishna**
Senior Engineer (Mentor)	**Technical Project Manager**
MS/ENF1, BGSW	**MS/ENF1, BGSW**

ABSTRACT

This study focuses on bringing the CFD methodology for oil-cooling simulation of traction motors. With a tremendous rise in electric vehicles, it is desirable to check the capability of an electric motor at different operating conditions using CFD simulation. The thermal management of an electric motor is very essential as it directly impacts the design parameters and life of the electric motor.

In this study, the CFD simulation has been carried out using Ansys fluent software to analyze the flow of oil inside a rotor shaft, the oil wetting area of the windings, and its effect on their temperature profile. Initially, the oil flow behavior in the hollow rotor shaft is studied using the pseudo-transient approach, and it is found that the flow distribution between the rear and front side nozzles is in the ratio of 0.91-1.08.

Additionally, transient simulation is conducted to capture the oil jet phenomenon on the end-space region, and the winding wetting area is computed. The total winding wetting percentage using the transient approach comes out to be 27%, which is 7% higher than that using the pseudo-transient method. Along with this, the mixed-time step coupling approach is used for extracting the contour of the temperature profile, which helps determine the temperature hotspot region of the motor components.

This study is intended to reduce the computational time required for the transient simulation of motor cooling. Simulating complex motor geometry using a multiphase model with a moving mesh approach makes it a complex physics to simulate, eventually increasing the simulation time. The methodology used in this study can reduce the simulation time using some additional features of Ansys Fluent, like PUMA and NITA techniques. The methods used in this study will be implemented on the actual geometry with the hairpin windings to compare the time duration of this approach with the traditional approach.

ACKNOWLEDGEMENTS

I would like to express my thanks and sense of gratitude to my supervisor, Dr. Vikrant Khullar and Dr. Rajesh Kumar Shukla for their guidance during my master thesis work. I also got many valuable learnings from them in better understanding of the subjects. I thank him for giving me their valuable time and suggestions which helped me to finish my work at right time.

It is my duty and proud privilege to acknowledge the kind of support and guidance that I have received in the duration of my internship at Bosch Global Software Technology. I want to thank my internship supervisor Mr. Nagesh Biradar, Senior Engineer and Mr. Anand Maheswaran, specialist CFD Engineer at BGSW Pvt. Ltd., for their consistent support and guidance throughout my internship journey. I want to thank Mr. Nagesh for providing me this opportunity to implement all the learnings that has been gained by me.

Furthermore, I would like to express my sincere gratitude to the Mechanical Engineering Department of Thapar Institute of Engineering and Technology for giving me all the learning opportunity that I have got in my master's course. Finally, I would like to express my sincerest sense of gratitude to my family for their support and love for me, without which this work could not have been possible.

TABLE OF CONTENT

List of Figure

List of Tables:

Nomenclature

μ	Viscosity [Ns. m^{-2}]
Q	Heat [J]
I	Current [A]
R	Resistance [Ω]
Ø	Scalar
ρ	Density [kg/m^3]
V	Volume [m^3]
u	Velocity in x-direction [m/s]
n	Normal vector
∇	Dell-operator
A	Area [m2]
D	Derivative
∂	Partial derivative
δ	Elemental thickness [m]
T	Temperature [K]
E	Enthalpy [Joule]
Δh	Grid cell [mm]
Δt	Time step size [sec]
C	Courant Number
U	Fluid velocity [m/sec]
N	RPM
ω	Omega
Re	Reynolds Number
ϵ	Epsilon

Abbreviation:

CFD	Computational Fluid Dynamics
IC	Internal combustion
BGSW	Bosch Global Software Technology
DPM	Discrete Phase Modelling
VOF	Volume of Fluid
MRF	Moving Reference Frame
SMM	Sliding Mesh Motion
NITA	Non-iterative time Advancement
SAE	Society of Automotive Engineer
EM	Electric motors
HTC	Heat Transfer Coefficient
LPM	Liter per minute
RPM	Rotation per minute
IPM	Interior Permanent Magnet
W	Watt
TEFC	Totally Enclosed Fan Cooled
NVH	Noise Vibration & Harshness
ANN	Artificial Neural Network
CAD	Computer added design
DC	Direct Current
AC	Alternating Current
EMF	Electromotive force
PMSM	Permanent Magnet Synchronous Motor
SST	Shear Stress Transport
CHT	Conjugate Heat Transfer
CFL	Courant–Friedrichs–Lewy
RPS	Rotation per Second
Vt	Tangential Velocity
PUMA	Polyhedral Unstructured Mesh Adaption
TUI	Text user Interface

CHAPTER: 1
INTRODUCTION

1.1 BACKGROUND

The demand of electric vehicle has increased drastically in recent times, as it has very high potential to reduce the carbon emission as compared to traditional IC engines. The performance of electric vehicles depends largely on the performance of electric motor. Electric motors used in electric vehicle will be running at high rpm to meet its requirement. At high rpm, electric motor will dissipate large amount of heat due to some losses, like joule losses, friction losses, eddy current loss, hysteresis loss etc. These losses result into high heat generation in the e- machines. So proper thermal management is highly desirable for achieving the optimum performance and reliability of the electric vehicles.

With the rise of electric vehicles, the cooling management of electric motors are the major area of research in the automotive industry. There are many losses in the motors which ultimately leads to heat generation. The electromagnetic losses include core loss in laminations, eddy current loss in magnets and copper loss in windings. So, the efficient heat management can overcome these losses and can reduce size, weight, and cost of the electric motor without affecting its performance. The oil-cooled electric motors are highly needed in high-power density traction motors, in which a hollow rotating shaft with nozzles is used to supply oil to various motor components as a design concepts. For effective cooling of electric motor, the shaft design optimization is very crucial for ensuring required flow distribution, this includes multiple flow rate, rotational speed and design parameters.

Many cooling topologies has been proposed in the past related to the cooling of electric motors. Out of which, the hollow rotating shafts with the oil pumping mechanism are the most crucial design for optimal cooling of the motor. The oil flowing in the hollow rotor shaft is to split up in the front and back side of the shaft. Then with the centrifugal action, the oil flows radially out of the shaft through nozzles fitted in the required direction on the shaft. This oil coming out of the shaft will splash on the windings surface will can reduce the winding temperature and the chance of creating hotspots. Also from the hollow shaft, oil can flow in the axial direction of the rotor lamination, which can cool the rotor as well as the magnets.

1.2 OBJECTIVES

This simulation study has been conducted in the simulation department of Bosch Global Software Technology (BGSW) using a CFD software Ansys Fluent 2022 R2 version. The CFD tool is used to study the heat transfer and fluid flow problems to avoid the high-cost experimental study using complex prototypes. Using accurate numerical methods, complex geometries with variable real time operating parameters can be analyses more precisely with lesser time and cost.

Few papers have been studied based on oil flow behavior in the hollow rotor shaft and the study of oil wetting percentage on the end windings with the mixed time-scale coupling approach in which similar study has been conducted.

This study focusses on developing the CFD methodology by using Ansys Fluent 2022R2 version, to perform three phases of simulation.

- To understand the oil flow behavior inside the rotating shaft.
- To compute the oil wetting area of the end windings
- To understand the mixed-time step coupling of fluid and solid domain.

The description of these phases of simulation are to be explained in the methodology section.

1.3 Cooling of Electric Motors:

There could be two ways for cooling the electric motors, one using indirect method in which coolant having the mixture of water and ethylene glycol in the equal proportion are made to flow on the stator housing. For this a required cooling channel is designed on the stator housing which cools the main stator windings through the means of conduction and convection.

The other way is direct cooling method in which a dielectric medium is made to flow inside the hollow rotor shaft, through which the dielectric medium (commonly called as oil), is splash or impinge on the end-windings through the nozzles fitted radially in the rotor shaft using centrifugal effect.

Two methods for removing heat from the electric motors are:

Indirect method: In this method, fluids are not in direct contact with the machines. In such a method, we need to design a cooling channel over the stator housing through which coolant or water is to pass through. Coolant from the coolant pump will enter the housing and flow in a defined coolant path over the stator housing. This will remove the additional heat generated into the motor by the main windings.

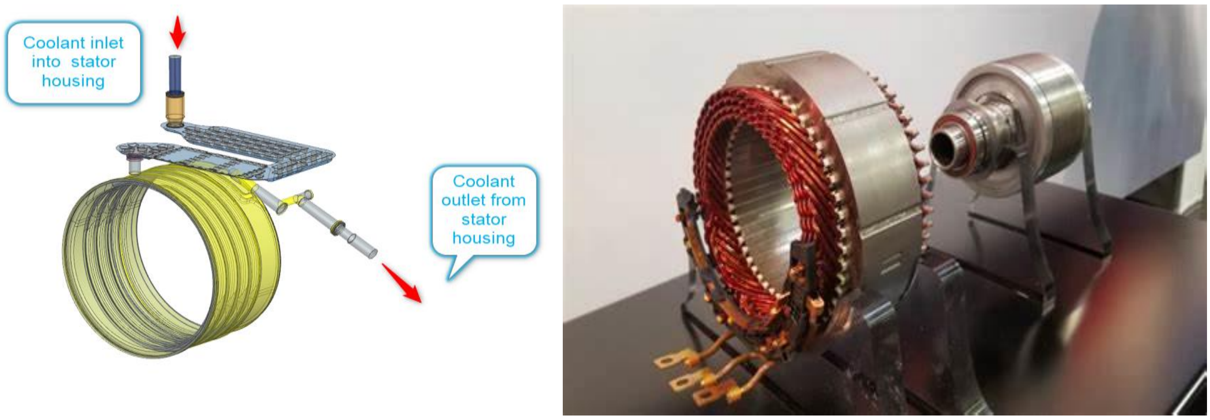

Fig.1 (a) Schematic diagram of coolant flow channel [Courtesy: Bosch], (b) picture showing the photograph of actual rotor and stator of the motor [21]

Direct method: In this method, dielectric medium is used as a cooling fluid to avoid short- circuiting. This oil (fluid) is passed through a hollow rotor shaft, this extracts the heat generated in the rotor due to magnet loss and friction loss. Magnetic loss is predominant due to magnets fitted into the rotor and friction loss due to rotation of rotor shaft at high rpm. So direct cooling of rotor shaft is important for sustaining the life of electric motor and to overcome the losses.

1.4 Simulation study

The Indirect cooling method is used in this simulation study in which oil is used as a dielectric medium and it is allowed to flow in the hollow rotating rotor shaft. From which oil would further pass through the nozzles fitted into the end of the shaft. This oil will be sprayed to the end windings, which constitute of approximately 30% of the total stator windings of the motor. Many researchers have worked on cooling of the rotor shaft- through different approaches. As stator windings are the major heat generating source of the motor. Determining the cooling methodology for end-windings is important. This paper focusses on the determining the simulation technique for effective cooling approach for end-windings. This oil gets sprayed to the end- windings and extract the heat generated from it, due to joule and core losses.

Many cooling topologies has been proposed in the past related to the cooling of electric motors. Out of which, the hollow rotating shafts with the oil pumping mechanism are the most crucial design for optimal cooling of the motor. The oil flowing in the hollow rotor shaft is to split up in the front and back side of the shaft. Then with the centrifugal action, the oil flows radially out of the shaft through nozzles fitted in the required direction on the shaft. This oil coming out of the shaft will splash on the windings surface will can reduce the winding temperature and the chance of creating hotspots. Also from the hollow shaft, oil can flow in the axial direction of the rotor lamination, which can cool the rotor as well as the magnets.

The end-winding cooling is required because the stator windings are the most heat generating source in the electric motor. And the end-windings consist of approximately 30% of the total length of stator windings.

For dissipating heat from the 30% of stator windings, the way is direct oil impingement on it.

For this we have the two approaches, one way is the oil flowing in the rotor shaft and splashing the oil on the end-windings using radial nozzles. This wets the inner part of the end-windings. The impact of gravity, the mass flow rate of oil inside the shaft and the rotational velocity of the shaft plays the major role in the amount of area getting wetted in the end-windings. Higher the rotational velocity of the shaft, lesser will be the impact of gravity on it and more will be the uniformity of the oil distribution on the end-windings. Whereas, lesser the rotational velocity of the shaft more will be the gravity impact which will only let the oil distribution in the direction of gravity impact. More the mass flow rate of oil, more will be the uniformity of the oil trajectory coming out from the nozzle tips. There will be less break-ups of oil or droplets formation in the end-windings region, which eventually increase the wetting area, heat the winding temperature. So higher the mass flow rate, higher will be the consistency of the oil trajectory. Hence, considering the effects of following parameters, we can simulate the domain without using DPM (discrete phase modelling) method, we can do the simulation using (VOF) method. Since the minimum oil droplets size would be larger the volumetric mesh size.

The other way is the splashing of oil through stator showers. The flow channel is designed such that the oil from the pump gets bifurcated based on the requirement using pressure valve. And the oil in the stator showed gets segregated and spitted equally in the two channels for left and right side of the end windings. Through that nozzles are designed for each stator shower which will splash the oil on the end-windings using gravity driven flow. Comparing the centrifugal driven flow and the gravity driven flow, the flow driven by gravity will splash more oil than the prior.

The oil is supplied in the rotor shaft and the stator shower through the same source. Pressure valve is fitted between the junction of both the circuit. Based on the requirement of oil and the drop of pressure, oil is supplied to the required circuit. The flow split-up of oil in the two rows of nozzles is essential for optimal cooling of motor. In this two-phase flow problem, the steady state solver accelerates the solution using moving reference frame approach. The parameters influencing the flow distributions are flow rate and rpm. The study has been conducted at different operating conditions and the methodology to setup the steady state VOF simulation for hollow rotating shaft has been explained. The CFD simulation is performed in this study which follows the finite volume method approach. In this approach, the flow equation solved are general transport equation, i.e., continuity, X, Y and Z momentum equation and general conduction equation (if energy equation is enabled).

The dielectric medium (oil) used here is known as Newtonian fluid, since the viscosity of oil used is not affected by any other factor other than temperature. As μ=f(Temp) only**.** The fluid can bear the shear stress at high rotational speed of shaft and no disintegration of oil will occur at this condition, because the viscosity of Newtonian fluid does not change with the shear stress.

Oil flow VOF simulation is performed using steady state and transient approach. The pseudo transient approach uses the moving reference frame (MRF) method, and the full transient approach uses the sliding mesh motion (SMM) method. Both the approaches are compared and found that the pseudo transient VOF solver can perform the shaft simulation 10-20 times faster than the transient approach. The transient method could be used for the oil splashing simulation and the winding wetting analysis as explained in the methodology.

The solution strategy used in this simulation study is that, initially oil flow is developed inside the shaft using pseudo transient MRF approach without mesh motion. Till the flow gets developed in the shaft and the mass imbalance graph gets Stabilized below the convergence limit. Then, the spray of oil jet on the windings are captured with transient sliding mesh (with mesh motion) approach and using the mesh adaption technique. Hybrid NITA solver and dynamic mesh adaption technique are utilized to enhance the solution accuracy with the reasonable simulation speed.

The electric vehicles used for heavy loading condition has high torque requirement. With rise in torque, more current supply is required in the motor. And the heat generated in the stator windings increases proportionally with the square of current flow. So, at high torque condition, more heat will be generated inside the electric motor due to accumulation of heat at the stator windings. Hotspots can be created due to this, which can corrode the coil of windings and can eventually decrease the motor efficiency. Whereas, at low torque and high rpm condition, higher will be the rotational velocity of the rotor shaft. At this condition, more heat gets accumulated in the rotor body which can demagnetize the magnets fitted in the rotor laminations for permanent magnet synchronous motor. So, at any loading condition the heat management is very essential for the electric motor.

At higher loading condition, when more torque is required through the motor the current passing through the windings will be high, which eventually increases the joule loss (Q= I^2*R). At this high torque condition, the winding temperature will increase. So, the higher cooling management is required for the windings. For cooling the main windings, the flow rate of coolant can be increased. And for cooling the end-windings, higher splashing of oil will be required on it. So, the stator shower valve will get activated and will flow more oil in this condition. And thus, remove maximum heat from windings.

At higher speed condition and low torque condition, rotor shaft will rotate at higher velocity. This can produce mechanical and magnetic losses. Since the magnets fitted in the rotor lamination can get demagnetized due to high rotational velocity. At this loading condition, the requirement of cooling is more for the rotor than for the stator. Hence the pressure valve fitted at the junction, will allow more oil to the rotor shaft. This way the oil cooling circuit operates at various loading condition and can reduce winding loss and magnetic loss.

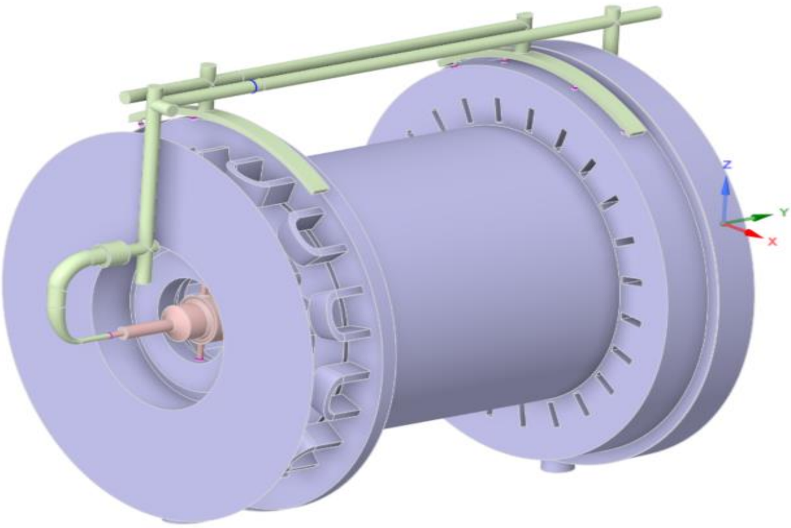

Fig.2 Diagram of oil circuit of electric motor

CHAPTER 2
LITERATURE SURVEY

2.1 Literature Survey

For the past few years, many researchers around the world have tried to understand and analyze the effect of liquid cooling of E-motors used in Electric vehicles.

A paper published in SAE's journal by Srinivasan, Yang.et al. (2020) [1] used the simerics software for computing the temperature field and the wetting area of the end windings of the electric motor. The study was based on CFD analysis of oil cooling of electric motors using oil flowing through the rotor shaft and splashing to the stator end windings using nozzle [1]. And other method through oil cooling directly through pouring on the outer windings using stator showers fitted with the funnels in it. This study was done using mixed time coupling using two-time steps for solid simulation and liquid simulation till the temperature field gets converged and validating the results using the conjugate heat transfer simulation by modelling entire the solid and liquid domain. The wetting area was compared for both the studies. The final temperature results were validated using the thermocouples used for determining the temperature field.

A paper by Boglietti et al. [2] showing the analysis of internal air-cooling effect on the end winding temperature with an experimental approach using suitable prototypes [2], showed that the end winding part overtemperatures decreases with increasing the inner air temperature. And it is concluded that, the graph of HTC vs inner air speed shows the linear dependency for a considerable speed range. Therefore, the internal ventilation is highly efficient for motor with more free space around the end windings. A study conducted by Kimiabeigi et al. [3] is conducted based on hollow-shaft cooling system [3], in which the coolant flows through the hollow shaft to cool it and to avoid rotor magnets in getting demagnetized. The effect of rotational velocity and the coolant flow rate has been accounted for the estimation of HTC. It is explained that the rotation in the shaft generates a destabilizing effect due to increase in the shear stress (caused by the wall rotation) which increases the heat transfer. It is also concluded that as the rotational effect directly impact the convective heat transfer coefficient, so the convective heat transfer coefficient can increase about 3.8 times at 4500rpm as compared to stationary case. A paper conducted by Boglietti et al. [4] deals with the analysis of internal air-cooling effects of temperature on the end winding with an experimental approach by using suitable prototypes [4]. The measurement results have shown that all the motor part overtemperatures decreasing with the increasing of inner air speed. And for a considered speed range, linear dependence of the heat transfer coefficients versus the inner air speed has been found.

The study conducted by Lee et al. [5] introduces an interior permanent magnet (IPM) motor that incorporates a forced cooling method through the use of cooling channels in the motor housing and a hollow shaft in the rotor. The researchers concluded that this cooling system has the ability to increase motor power by enabling high motor speeds with an enhanced cooling effect. As a result, the IPM motor is deemed suitable for high-speed applications such as electric vehicles. During the experiment, the proposed IPM motor demonstrated significant temperature reductions compared to both an air-cooled motor and a liquid-cooled motor after an 80-minute operation. Specifically, the temperature of the coil in the proposed IPM motor decreased by 50% compared to the air-cooled motor, and by 38% compared to the liquid-cooled motor. This temperature decrease leads to an increase in current density within the motor. Consequently, the reduction in temperature helps minimize eddy current losses when the coolant flows through the hollow rotor shaft of the IPM motor while operating at high speeds.

The study conducted by Nonneman et al. [6] has been done which compare four cooling topologies to determine their effectiveness in heat transfer and minimizing permanent magnet temperature. Increasing rotational speed was found to enhance heat transfer, while the influence of mass flow rate was minimal. Rotor jet cooling was identified as the most effective technique, as it facilitated forced convection near the rotor iron, resulting in efficient cooling. Hollow shaft liquid cooling and rotating heat pipe cooling exhibited similar temperature distributions in motor components.

Assaad et al. [7] conducted an experimental study on a new design for an oil-cooled induction motor. The proposed design suggests replacing the external fan on the shaft with a hollow shaft containing holes on its surface. These holes allow the oil coolant to be directed inside the motor, specifically targeting the stator end-windings and rotor end-rings for cooling purposes. Multiple designs were compared at the motor's critical operating point of 10000 rpm/40 kW. The first design involved oil cooling through a hollow shaft with a fan, while the second design added holes in the shaft for oil projection onto critical areas. It was found that without these holes, the temperature exceeded thermal limits by three times. In terms of power output, compared to a traditional TEFC motor with a power rating of 19 kW, the continuous power significantly increased to 37 kW with the addition of oil injection at a rate of 3 liters per minute. Similarly, compared to the same traditional TEFC motor with oil injection at a rate of 3 liters per minute, the continuous power increased by 19 kW, although mechanical losses also increased by 1 kW.

An article discusses various cooling methods for both present and future traction motors [8]. It evaluates these methods and proposes that employing an end winding jet impingement or spray cooling design could be an effective and uncomplicated solution for cooling the end winding.

The cooling topologies of electric machines based on the development results of the parts such as lubricating oil and motive seal of electric vehicles was presented in a paper Gundabattini et al. [9].

Coolants was used in cooling jackets for indirect cooling and oil enter in the internal part of the motor to cool the hot spot directly. Also, it was mentioned that the spray of cooling fluid can cause the coil erosion and the adverse effects of the oil-air mixture. The shaft is likely to have a dynamic imbalance, leading to NVH problem. Also, the limited position of the injection openings can cause an inadequate cooling on the stator windings.

An experimental study on oil spray for end winding thermal management by Wang et al. [10] was conducted using artificial neural network (ANN) model for better prediction of HTC, indicates that the oil spray significantly reduces the winding temperature. It was suggested that with higher oil temperature and higher oil flow rate, better cooling performance and better uniformity of temperature for slot windings can be achieved. Since with higher oil flow rate, more oil is pumped to the surface of end windings, thus the end winding is well covered and wetted by the oil. A s a result, more heat is dissipated by the oil due to its larger heat capacity.

A study has been conducted by Chen et al. in which impinging jet was utilized to decrease the stator end winding temperature of electric motor using inverse method in numerical simulation [11] and validated the temperature results using infrared imaging at three testing configurations. As infrared camera can measure the winding temperature with influencing the heat transfer or the flow behavior. The HTC was calculated using inverse method and the results shows that, oil flow in the internal surface on end windings gives better cooling performance.

A study based on Taguchi analysis by Garud et al. [12] was conducted for evaluating the effect of some influential factor on heat transfer performance of oil spray cooling system in electric vehicle using three different nozzle type. It was concluded that flow rate and heat capacity impacts maximum on heat transfer coefficient and spray power consumption. Also, the full cone nozzle shows lowest surface temperature and maximum heat transfer coefficient compared to spiral and hollow-cone nozzle.

2.2 Research Gap:

Few research papers have been studied and their approach and their findings are mentioned. Based on CFD simulation of the oil splashing on end windings, very few papers are published. The nature of flow of oil through the nozzle fitted on the rotor shaft, their effect on heat dissipation and area of end-windings covered during the oil splashing are yet to be determined.

2.3 <u>Problem Statement:</u>

To cool the end windings of the stator through oil impingement/ oil splashing through a nozzle fitted into the hollow shaft. Also, to determine the winding wetting area and the amount of heat extracted from the end windings.

2.4 <u>Research Objectives</u>:

- To develop a model and to simulate the flow of fluid in the rotating rotor shaft.
- To analyze the oil flow inside the hollow rotor shaft at different mass flow rate and rpm
- Computation of oil wetted area by oil splashing over the end windings and to analyze the impact of oil splashing on the end-windings.
- To come up with a numerical methodology for effective heat management of the stator end-windings for the traction motors with less computational time.

2.5 <u>Work flow of the Simulation study:</u>

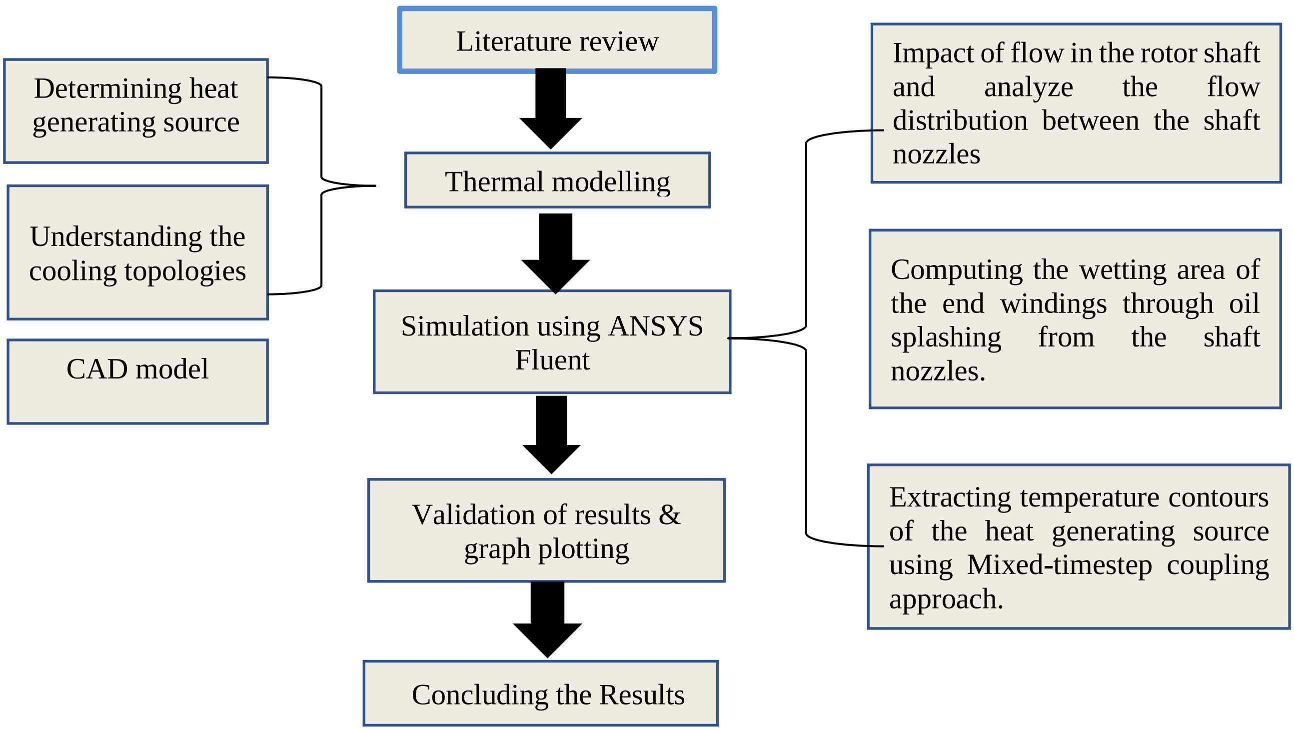

Chapter:3

Problem Definition and CFD Modelling

3.1 Theory of Electric Motors:

An electrical machine which converts the electrical energy into the mechanical energy, is known as electric motor. For this energy conversion, electric motor usually interacts with the magnetic field of motor to the electric current of the windings to generate torque that is to be supplied to the rotor shaft. In a vice versa process, this device can act as a generator that will convert the mechanical energy to the electrical energy. Electric motors can be powered by DC sources, like batteries, rectifier or by alternating sources like power grid, inverter or electric generators. Studies suggested that electric motors are over 95% efficient and conventional internal combustion engines are below 50% efficient. As the electric motors have high power density, compactness, high durability, efficiency, light in weight and can provide instant torque at wide range of speed and can operate using renewable energy source without carbon emission. Generally electric motors are of different types, the one used in this work is permanent motor synchronous motor. In this type of electric motor, the rotor contains the permanent magnet which aims to transmit the mechanical force as rotational motion using the rotor shaft to the external components. While windings are placed on the stator slots in a concentrated geometry through which electric current is supplied to generate electromotive force in the electric motor.

The air gap is a crucial gap between the rotor and the stator, which should be sufficient enough to avoid the contact between the two domains during rotor rotation, and to maintain the motor efficiency and performance. As more the air gap between the rotor and stator more power would be required to magnetize the rotor magnets and lesser the airgap more will be the chance of contact between the rotor and stator which can cause the damage to motor components [14].


Fig.3 (a) Electric motor with stator and rotor components [Source: bosch-mobility.com] (b) Concentrated winding configuration [Source: electricmotorengineering.com] [14]

The electric motor driven by alternating current is majorly if two types, the induction motor and the synchronous motor. The induction motor is an asynchronous motor in which there is a small difference in speed between the magnetic field produced by the stator and the shaft speed of the rotor. The difference is called slip which induces AC current in the rotor. The torque cannot be produced in the induction motor where considerable slip doesn't exist. Whereas the synchronous motor does not depend on and slip induction for operation and produces rated torque at synchronous speed using either permanent magnets or independently excited rotor windings.

3.2 Permanent magnet synchronous motor

In synchronous motor the speed of rotor is same as the speed of rotating magnetic field of the motor. The stator is similar to that of induction motor consisting of stator slots with windings, usually three-phase located in slots around the inner periphery. While the rotor contains permanent magnets mounted in the slots of rotor laminations instead of wounded field windings of rotor used in induction motors. In synchronous motor, the alternating current supplied to the stator windings produces a sinusoidal EMF which rotates the rotor at the same speed, whereas the induction motor rotates the rotor at somewhat slower speed than the stator field.

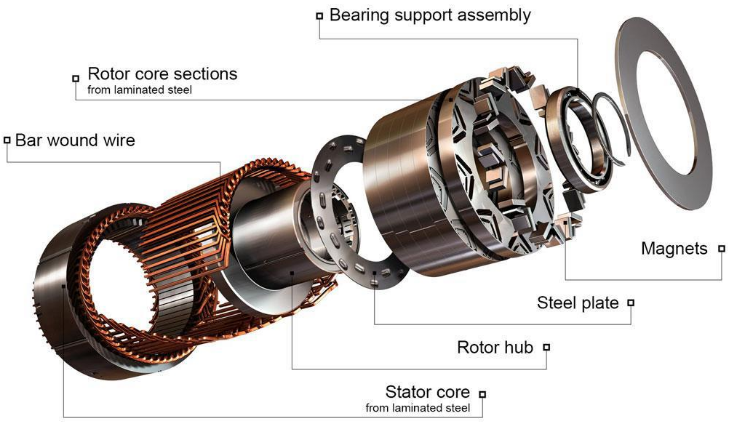

Fig.4 Permanent Magnet synchronous motor components [20]

The stator consists of armature windings in which the voltage is generated and the only difference in this type of motor is that the rotor doesn't have field windings, it has the permanent magnets to create field poles. Due to high permeability of permanent magnets, it is made up of samarium cobalt, medium iron and boron. The mounting of permanent magnets can be in two ways, surface mounted or interior mounted PMSM motor, as depicted in the below figure. The surface mounted magnets provide a uniform air gap. It is suited for high-speed application and it is not robust, as it has no reluctance torque. While the Interior mounted magnets are robust which gives reluctance torque and it is suitable for high-speed application.

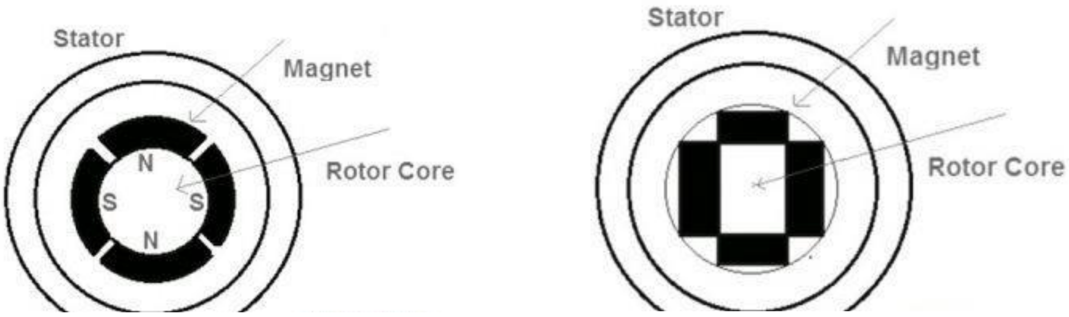

Fig.5 (a) Surface mounted (b) Interior PMSM [22]

3.3 Need of Thermal Management:

The efficiency of an electric motor is directly affected by the losses present in the electric motor. Electric motors running at high rpm will dissipate large amount of heat due to some losses, like joule losses, friction losses, eddy current loss, hysteresis loss etc. These losses result into high heat generation in the e- machines. So proper thermal management is needed to maintain the life cycle of the electric motor and to avoid the demagnetization of magnets fitted into the motor.

Heat is generated in the e-machine by electromagnetic and mechanical losses. Losses distribution highly depends on machine topology, loads and supply conditions. Joule losses are generated by electric currents in the windings. Core losses include hysteresis loss, eddy current and stray losses, they are in the laminations of the machine. Magnet losses are due to eddy currents; they can be high in concentrated winding topologies with surface magnets. [17] Mechanical losses include friction and windage losses (friction in bearing, aerodynamics friction and drag). The resistance of winding on the flow of current determines the joule losses. Iron loss depends on the speed of motor and on the motor flux density. Iron losses are of two type, Hysteresis loss and Eddy current loss. The eddy current losses are caused by the change in magnetic flux in the conducting body, so thinner lamination is required to reduce this loss. Whereas the hysteresis losses are caused by energy loss from the redirection of magnetic domain in the steel.

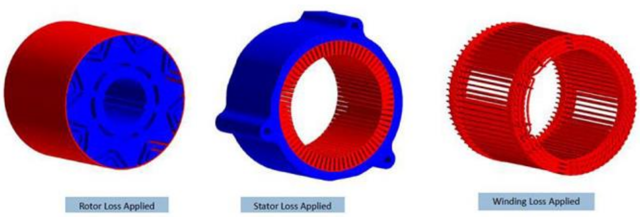

Rotor Iron Loss	Stator Iron Loss	Winding Loss
0.17	0.4	0.43

All Values are scaled with a reference heat loss value

Fig.6 The fraction of heat distributed between the three zones of motor, Chiranth et al. [1]

All these losses tend to rise the temperature and accumulate heat in the motor components. With rise in temperature internal magnets, winding insulation and bearing gets degrade as it is the main heat source in permanent magnet synchronous motor. For maintaining the life of motor components, efficient heat dissipation is very necessary. Study has been conducted in which losses are calculated in terms of percentage as shown in figure [1]. Out of which the winding loss are highest at around 43%. This study focusses on cooling of end-windings which is not in direct contact with the cooling channel of the stator housing. The end windings are approximately 30% of the length of total winding.

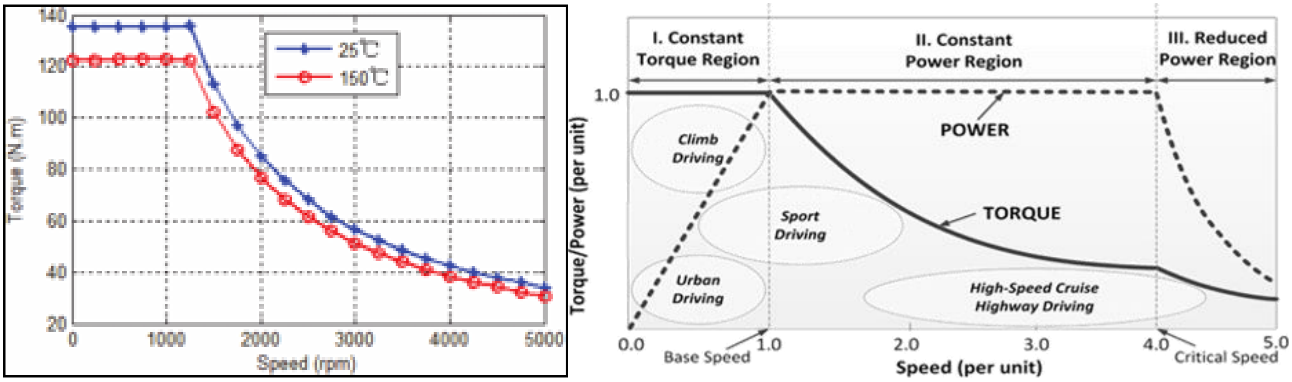

Fig.7 (a) Torque vs speed graph at different temperature [15] (b) Variation of speed at difeerent torque condition [16]

3.4 Governing Equations of Fluid Flow and Heat Transfer

CFD is a science of predicting fluid flow motion, heat and mass transfer, and similar phenomenon by solving differential equations which govern this process using a numerical method. The Ansys Fluent software is based on the finite volume method in which the domains are divided into finite control volume for which discretized governing equations are solved. CFD is primarily based on governing equations of fluid dynamics that represents the conservation law of physics [18].

The governing equations are:

- Mass conservation (based on continuity equation)
- Momentum conservation (based on Newton's second law)
- Energy equation (based on first law of thermodynamics

The governing equations are explained below:

1. **VOF (Volume of Fluid fraction) Equation:**

$$\frac{\partial \alpha_l}{\partial t} + \mathbf{V} \cdot \nabla \alpha_l = 0 \qquad (1)$$

For each phase, a variable i.e. the volume fraction (α_l) of the phase is defined in all the control volumes. In each control volume, the sum of the volume fractions of two phases is unity.

$$\alpha_l + \alpha_g = 1 \tag{1a}$$

Where α_l and α_g denote the volume fraction of the oil and air respectively.

2. **Continuity Equation:**

This equation is based on conservation of mass, based on balance between the amount of fluid entering and exiting the domains.

$$\nabla \cdot (V) = 0 \tag{2}$$

3. **Momentum Equation:**

This equation is based on Newton's second law, which states that the rate of increase of the momentum is equal to the sum of the forces on a fluid particle.

$$\frac{\partial}{\partial t}(\rho \mathbf{V}) + \nabla \cdot (\rho \mathbf{V}\mathbf{V}) = -\nabla p + \nabla \cdot [\mu(\nabla \mathbf{V} + \nabla \mathbf{V}^T)] + \rho \mathbf{g} + \mathbf{F} \tag{3}$$

Where, **V** represents the velocity vector, p is the pressure and **g** is the gravitational acceleration. The Navier-Stokes equation is dependent on the volume fraction of both the phases through the properties: density ρ and dynamic viscosity μ.

Where, the mixture properties are defined by the following equation,

$$\rho = \alpha_l \rho_l + \alpha_g \rho_g \tag{3a}$$

$$\mu = \alpha_l \mu_l + \alpha_g \mu_g \tag{3b}$$

$$k_{eff} = \alpha_l k_l + \alpha_g k_g \tag{3c}$$

4. **Energy Equation:**

This equation is based on First law of Thermodynamics.

$$\frac{\partial}{\partial t}(\rho H) + \nabla \cdot (\rho \mathbf{V} H) = \nabla \cdot (k_{eff} \nabla T) \tag{4}$$

H is the total enthalpy, k_{eff} is the effective thermal conductivity, T is the temperature. It may be noted that a single Navier-Stokes equation and a single energy equation are solved throughout the computational domain for both the phases.

3.5 <u>Multiphase Model</u>

The multiphase model is used to simulate the phase interaction between the different phases or state. It can also simulate the phase interaction of different chemical composition within same phase. In terms of CFD, the phases are distinguished by its certain properties not by its state of matter.

The Volume of Fluid (VOF) model is used in this multiphase model, to model two fluids (oil and air) with a defined interface. VOF is not appropriate if the interface length is small compared to a grid cell length. The accuracy of VOF decreases with interface length scale getting closer to the computational grid scale. The VOF model is generally used to compute a time dependent solution, but it is possible to perform a steady state calculation. A steady state VOF calculation is sensible only when your solution is independent of the initial conditions and there are distinct inflow and outflow boundaries for a individual phase.

In volume fraction parameter, explicit or implicit formulation can be used. In explicit scheme, the solution at the time step n+1 is calculated using the known values of solution at time n. Whereas in implicit scheme, the solution at n+1 time step is calculated using the unknown values of solution at time n+1. Thus, explicit scheme gives more accurate result at higher computational cost. While the implicit scheme can give comparatively faster results at lesser computational time. So, the formulation is chosen based on the requirement of simulation. In this study, implicit formulation is selected which allows faster solution with reasonably good accuracy.

3.6 <u>Courant Number</u>

In a CFD simulation, the Courant number broadly indicates how much the information travels (U) across a computational grid cell (Δx) in a unit of time (Δt). Courant number is used in transient simulation. For Explicit scheme $C \leq 1$, as flow should not travel over more than one grid cell during a time step. If courant number is greater than 1, it means that the information propagates through more than one grid cell at each time step, making solution inaccurate and it cause divergence.

$$C = \frac{U\,\Delta t}{\Delta x} \tag{5}$$

Where,

- U is the fluid velocity.
- Δt is the time step.
- Δx is the grid size.

In **explicit scheme**, the solution at the time step n+1 is calculated using the known values of solution at time n. Whereas in **implicit scheme**, the solution at time n+1 is calculated using the unknown values of solution at time n+1.

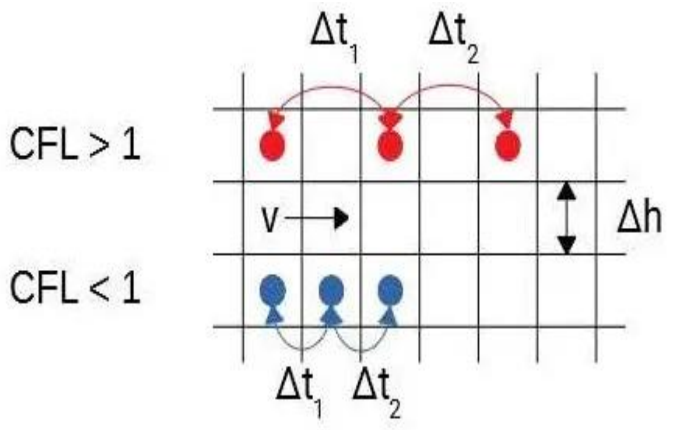

Fig.8 Visualization of the Courant number and the CFL condition on a computational grid [19]

3.7 <u>Approach for time step calculation</u>

If Ω=4000 rpm, (=66.67 rps), the nozzle moves by 1 degree of rotation in about 4.167 e-5 seconds, therefore this could be used as a reference time for selecting the time step.

$$\text{Time step } (\Delta t) \leq \frac{1}{\text{N (in rpm)}*60} \qquad (6)$$

Alternatively, we can consider the diameter of the rotating shaft and calculate the linear speed of the tips (Vt). If we assume the diameter of 23mm, Vt comes to be 4.817m/s. And with a time-step of 4.0e-5 seconds, the tips would cover about 0.24 mm of mesh size.

$$\text{Time step } (\Delta t) \leq \frac{\text{mesh size } (\Delta x)}{\text{Linear velocity (Vt)}} \qquad (7)$$

The adaptive time step strategy requires the definition of maximum allowed courant number. It adjusts the time step to meet the requirement.

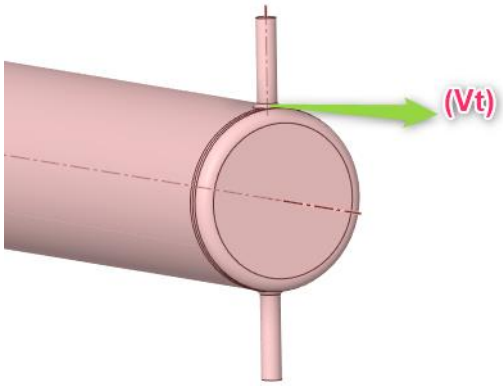

Fig.9 Pictorial representation of rotation of shaft

3.8 <u>Adaptive-type Transient settings:</u>

The setting used in adaptive-type transient simulations are as follows:

- Global courant number: It is the maximum limit of courant number.
- Number of time steps: Maximum time steps after which the time step size start varying.
- Initial time step size: Time step size for fixed time steps.
- Total time: Total physical time for simulation.

3.9 <u>Automatic Mesh Adaption technique</u>

Polyhedral Unstructured Mesh Adaption (PUMA) is the automatic mesh adaption technique, used for refining the mesh dynamically in a simulation. This scheme in Fluent enables you to start from a coarse mesh and dynamically refine high-gradient regions. Without this we used to manually decide the mesh size to accurately capture the important areas but also keep the total cell count manageable. With this it simultaneously increases the simulation speed and the accuracy of the solution. By automatically refines the mesh zone that is our area of interest and simultaneously coarsen the mesh which is not our area of interest.

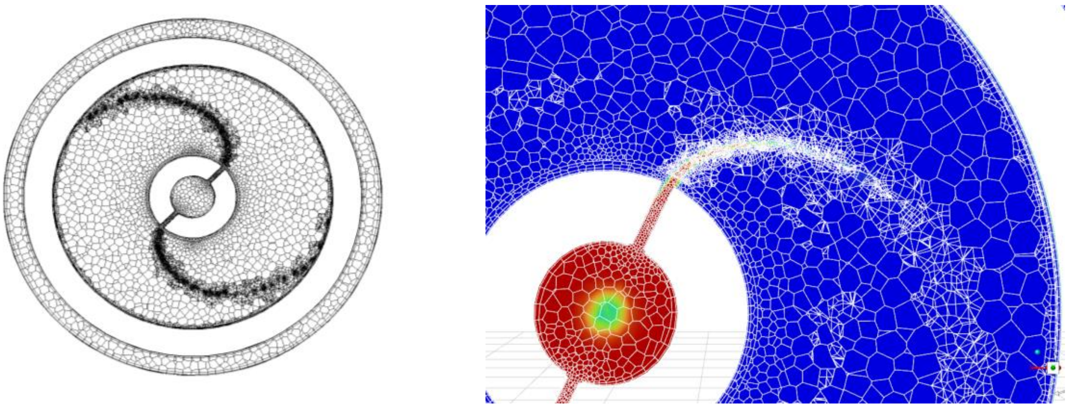

Fig.10 (a) PUMA enabled in mesh contour (b) Mesh refinements on oil trajectory

3.10 <u>Hybrid NITA scheme:</u>

NITA stands for non-iterative time advancement. This method is introduced in Fluent, for speeding-up the transient run. Transient run approach is used for capturing the oil trajectory from the shaft nozzles and the end-windings. Also, for evaluating the wetting area percentage and the location of maximum wetting zone. This approach uses sliding mesh motion in which the mesh is allowed to rotate for evaluating the actual scenario. The moving mesh approach require more simulation time and high computational expense. Hybrid NITA is recommended when using VOF method for getting robust solution at a cost of speed. This method is suitable for compressible, non-Newtonian or high viscosity ratio flow.

In adaptive type transient simulation, the number of iterations varies with variable courant number due to various parameters like, velocity speed-up or mesh size variation in a domain. These parameters decide the number of iterations to be perform in a time step, which eventually increase the computational time.

Non-iterative time advancement performs a fixed number of outer iterations within a time step, along with these sub-iterations are performed and thus it accelerates the transient simulation. The global courant number limit and the velocity limit is applied, if that limiting value is reach at any time-step, the number of iterations will increase to 5 in a time step. Thus, it reduces the chance of divergence in transient simulation and enhances the convergence stability.

3.11 Comparison between Simple iterative, Default Nita and Hybrid Nita scheme:

Default NITA:

It solves one outer iteration per time step, and it will solve more sub-iterations for each equation (continuity, u, v, w etc.….). Default Nita was not very robust.

Default Nita speed-up the transient run by 4x. But it was inaccurately speeding up the simulation.

Hybrid NITA:

Hybrid Nita speed-up the simulation runs with accuracy.

It is a combination of default Nita scheme and basic iterative scheme. Instead of 1 outer iteration, it will do 2-3 outer iteration (2 for aggressive and 3 for conservative) for each time-steps.

Lesser sub-iterations will be required and will get better coupling between the equations.

As compared to iterative solver, hybrid-Nita could speed up from 2x-4x.

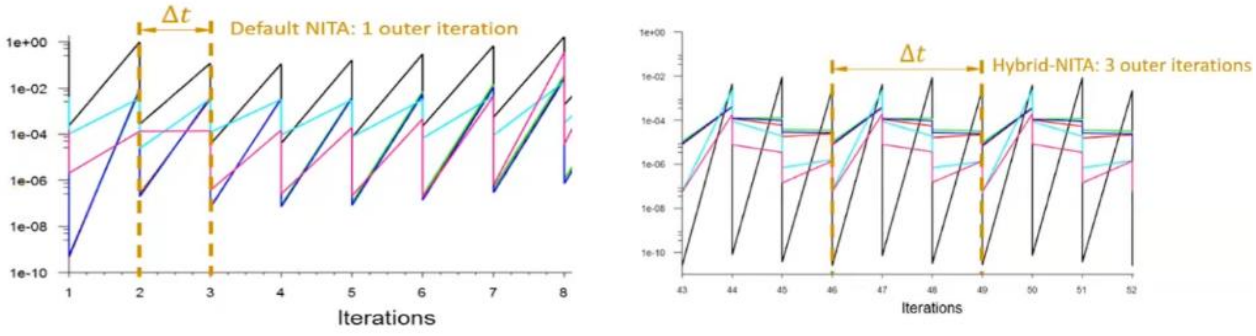

Fig.11 (a) Default NITA (1 iteration per time step) (b)Hybrid NITA (3 iteration per time step) [Courtesy: ANSYS]

3.12 Mixed time step coupling

Fluid domains consist of oil circuit, fluid extracted hollow rotor shaft, end-space region, rotor oil-air volume, stator showers. Solid domains consist of hollow rotor shaft, hollow oil inlet pipe, rotor laminations, stator laminations, coolant cooling channel, housing…etc. The regions apart from fluid extracted domain in the complete geometry is selected as solid domain. The solid and fluid simulation are conducted separately using their respective domains.

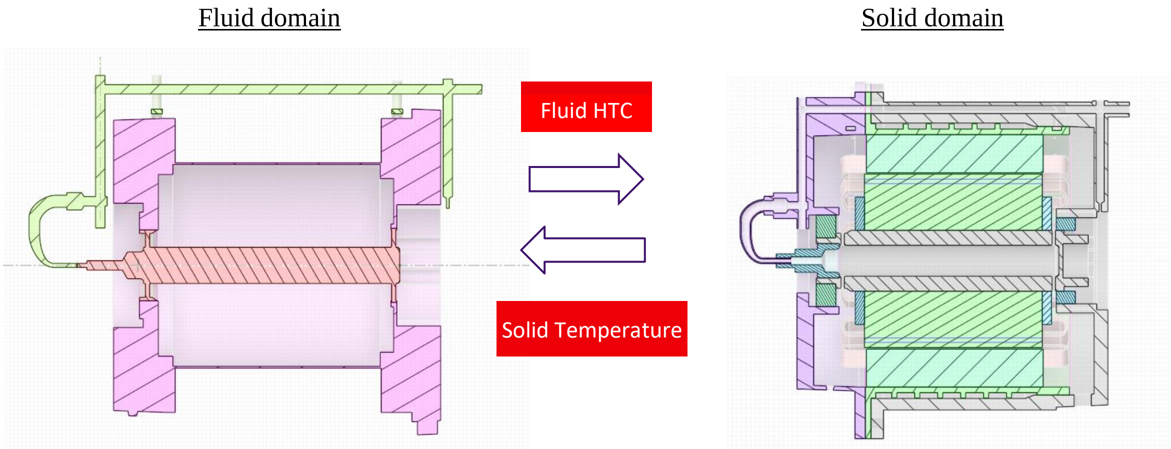

Fig.12 Pictorial representation of mixed- time step coupling approach for conjugate heat transfer method.

The fluid domain is the volume extracted domain of oil, the domain consisting of the region where oil is supposed to flow. The volume extraction tool of space Claim creates a fluid volume based on the volume enclosed by a single solid body. For the Conjugate heat transfer model, the solid and fluid simulation is conducted separately as taken from the SAE's reference paper by Chiranth et.al. [1]. Simulation is conducted separately since the solid and fluid has different thermal inertia, so mixed time scale coupling approach is used in which in which we specify two difference time-step size for solids and fluid domain. Due to higher thermal inertia of solid domain, it can take more time to reach the thermal equilibrium, whereas the thermal field of fluid domain can take more time to reach thermal equilibrium. So, it is suggested in the CHT simulation that the time-step size required for fluid domain should be one hundredth of that of the solid domain, because within smaller time duration there will not be any significant change in solid temperature.

Initially in mixed time step coupling approach, the HTC and the reference temperature is calculated in the fluid simulation, that temperature field data is mapped in the simulation using solid domain. Then, the pseudo transient solid simulation using mapped data is performed and temperature field is computed, and these results are mapped back to the simulation using fluid domain. This approach is repeated till the heat flux between the two domains are balanced and no further deviations are observed between the results.

CHAPTER :4

CFD Methodology

4.1 Overview of Methodology used in Ansys-Fluent:

This study focusses on developing a numerical methodology for cooling the end-windings of PMSM motor using CFD simulation. For computing the temperature field and hotspots of windings mixed-time scale coupling is used, in which the solid and fluid domains are simulated separately. Initially, with a reference temperature of the fluid-solid interface, the fluid simulation is performed. The temperature and the HTC values are calculated from the fluid simulation and mapped to the solid simulation. Similarly, the temperature and HTC value are calculated from the solid simulation and are mapped back to the fluid simulation. The temperature values are compared and this iterations of mapping the results on the other simulation are continued till the deviation gets stabilized. The stabilized temperature value is computed and hence the heat transfer coefficient and the hotspot temperature can be determined.

For performing simulation with energy equation, it is needed to compute the wetting area of the end-windings by the oil splashing from the shaft nozzles. This simulation is performed using the transient method with a sliding mesh motion as a cell zone condition, for accurately capturing the oil trajectory and the wetting regions of the end-windings. The shaft is provided with SMM, and the rotor parts are considered without rotation with MRF approach. With this the oil- air mixture flowing in the rotor laminations through the duct, can be captured. PUMA is enabled for refinement of mesh in the region of oil trajectory, and hybrid Nita is used to enhance the transient simulation speed. The winding wetting percentage using the iso-clip greater than 0.5 oil fraction for wetting area of both side windings with are computed. The wetting percentage for both side of end-windings are compared for transient and pseudo transient simulation. The extracted results are further used for CHT simulation.

For computing the wetting area using transient simulation, shaft simulation is to be performed prior using the pseudo-transient method. The oil flows in the hollow rotating shaft at certain rpm, and oil comes out from the nozzles fitted in the radial direction. Oil flows out from the nozzle with the centrifugal force due to the shaft rotation. Then the oil splashes the end-windings. So, before the transient simulation using mesh motion, the pseudo-transient simulation is to be performed for the shaft simulation. The moving reference frame is used as cell zone condition for the steady state simulation, in which shaft has not given any mesh motion and the effect of oil air flow is monitored inside the shaft. The mass imbalance within the inlet and outlet sections of shaft are monitored till the mass imbalance reaches below 5%.

4.2 Description of Geometry

A complete diagram of motor geometry in a mid-shaft plane is shown in figure. It consists of two different cooling channels. One is the indirect cooling in which coolant in a mixture of water and glycol is used in equal proportion to flow in a cooling channel designed on the stator housing.
Other is the direct oil cooling in the motor. In which two oil circuits are placed, direct oil flowing in the rotor shaft through inlet pipe and spraying on the end-windings through nozzles fitted radially in it. The other approach in oil-cooling circuit is splashing oil in the end-windings through stator showers. This would be a gravity-driven flow. With these two approaches of oil-cooling, we can cool both the inner and outer part of the end-windings. The shown cross-section view of the geometry shows the rotor shaft with lamination, stator lamination in the system housing and the cooling channel which consist of coolant channel, shaft oil circuit and stator shower oil channel as discussed.

There are 5 zones in the used geometry:

- *Oil circuit*: It contains the oil inlet passage for shaft and for stator shower.
- *Stator shower*: Oil showers bifurcated into two side of end windings
- *Fluid-rotor-volume*: It contains the rotor, rotor stacks and the magnets.
- *Fluid-shaft-oil*: It contains the hollow rotor shaft.
- *Fluid-air-volume*: Contains end windings and outer housings.

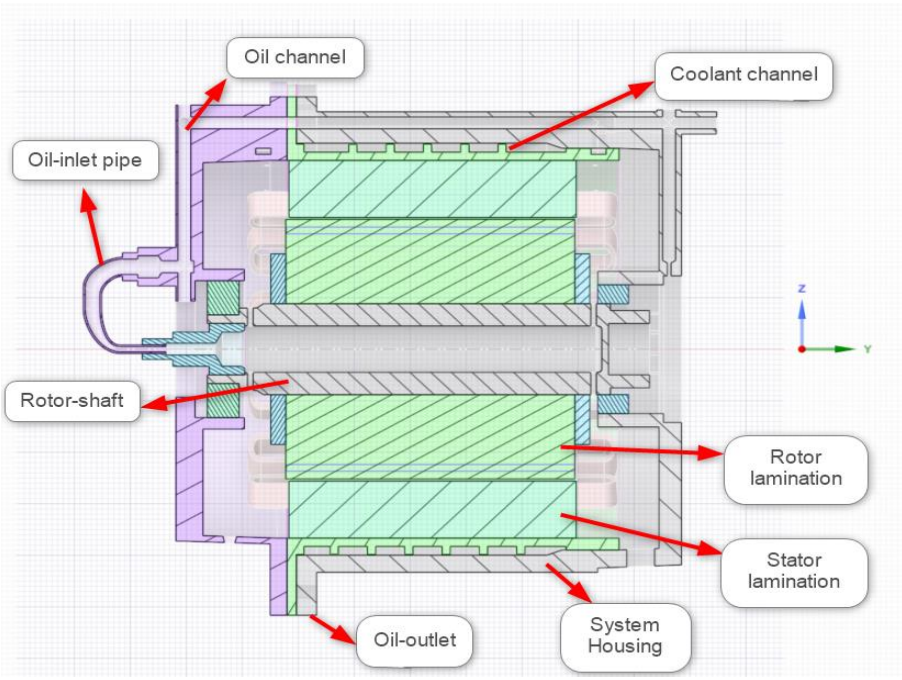

Fig.13 Schematic diagram of fluid domain in a cross-section view

4.3 Simplified model

A simplified geometry of electric motor having hollow rotor shaft with oil inlet, stator windings (including the end-windings), the housing covering the rotor stack and windings. In this simplified model of oil flow, stator showers are included, which pour the oil to the end-windings with the gravity driven flow. The oil circuit is given as two inlet source of equal mass flow rate, out of one flow in the rotor shaft and other flows through the stator shower. The oil entering in the hollow rotating shaft dissipates heat from the rotor shaft and magnets attached on the rotor lamination. The radial and tangential velocity dominates inside the hollow rotating shaft due to the centrifugal force. Due to which oil comes out from the nozzles fitted radially in the shaft, as shown in the cross-sectional view of the geometry. The oil coming out from the nozzles, splashes on the inner part of 2003end-windings. The oil entering the stator shower flows at high loading condition, and it is a gravity-driven flow.

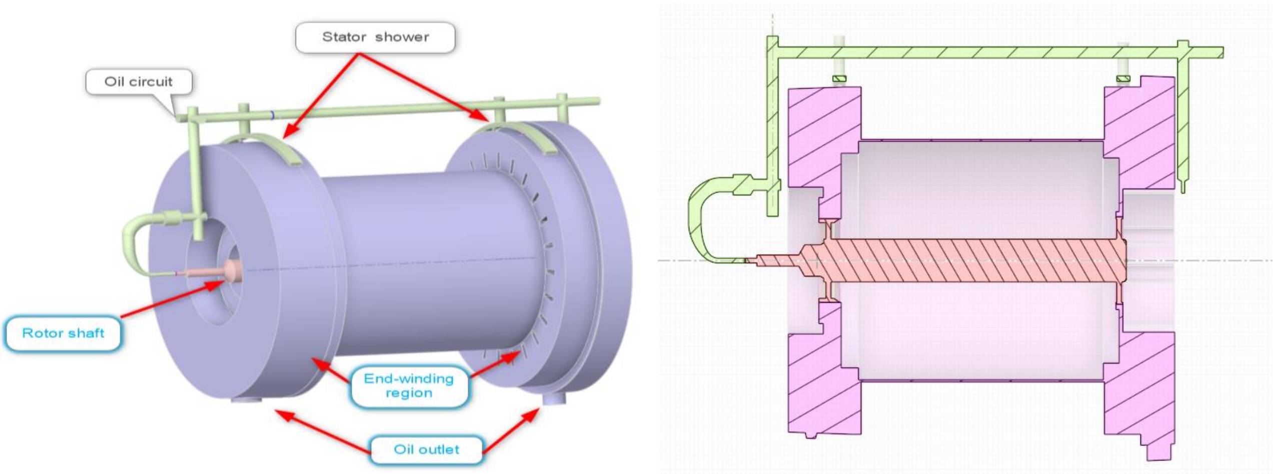

Fig.14 (a) Simplified motor geometry with the oil-circuits (b) Cross-section view of motor geometry

The simplified geometry is taken in Ansys Space Claim 2022R2 version of Ansys software. The basic modelling and clean-up of geometry are done using design commands in this software. This analysis tool focused on repairing, preparing, and optimizing the CAD model. The clean-up task is done before any simulation to get the uniformity in mesh and to avoid skewness in the structure.

The need for repair a geometry is to prevent from creating disconnected or corrupt geometry or to avoid missing faces, sharp edges, and meshing issues. The extra edges and curvatures are removed from the structure based on the area of interest to avoid the higher mesh count which eventually leads to higher computational cost and time, which needs to be reduced.

A cell zone is created in the periphery of shaft nozzle between the end space region and the shaft nozzle tip. These zones are required to create in simulation for accurately capturing the oil flow in the end space region. Since, the shaft has given the sliding mesh motion and the end-space region is not provided with any mesh motion. This will create a mesh interface between these two regions. So, when shaft will be rotating the interface will not rotate with the shaft. So, that oil trajectory gets captured when oil comes out from the nozzles.

4.4 <u>Geometry of the rotor shaft:</u>

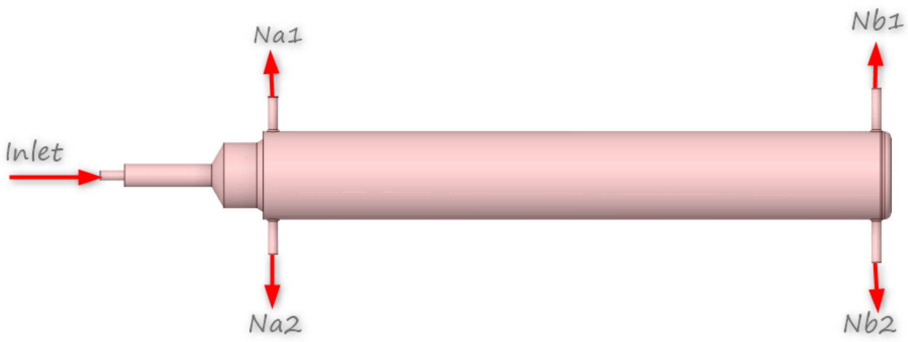

Fig.15 Front view of rotor-shaft with nozzles

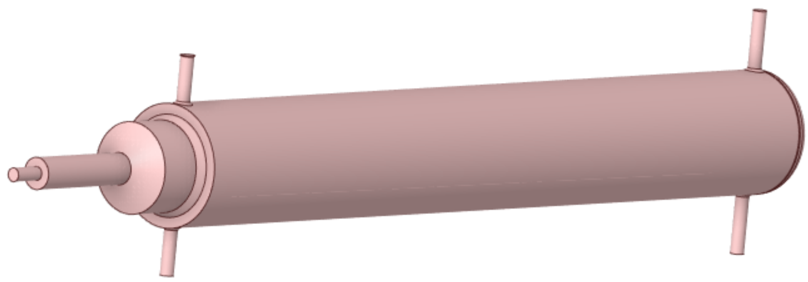

Fig.16 Isometric view of rotor shaft with nozzles.

<u>Geometry Description</u>

The e-motor shaft is a hollow shaft design. The shaft has axial opening at B side to receive oil from transmission. It has radial holes on both A/B sides to splash oil over motor end windings for cooling purpose. A pictorial illustration is shown below for e-motor shaft design. There is a leakage zone near the shaft inlet and two axial nozzles for the lubrication of transmission parts (not included in this geometry).

4.5 Meshing Methodology

The meshing procedure starts with importing the cleaned geometry using space claim in a watertight geometry workflow. Using this workflow perform sophisticated meshing which includes innovative poly-hexacore meshing algorithm, for high quality boundary layer mesh generation and parallel meshing. With this simplification, it can enable user to complete all stage of CFD simulation from meshing to post-processing in a single window.

After importing the CAD model in, we provide local sizing which includes face size, body size, body of influence, curvature, and proximity. We provide the sizes using approximation based on the complexity of geometry, so that the meshing would neither be coarser nor finer. Face size is provided on faces defined in named selection, body sizes are provided on the entire zones. Body of influence is an imaginary body that is created to change the mesh of specific area of interest without changing the overall mesh size.

In surface mesh generation, maximum and minimum mesh size is to specify with the growth rate value, which indicates the rate at which the mesh size vary in the structural domain. Then a size function having curvature and proximity size function needs to specify. The curvature size function is used for refining the surface mesh based on the underlying curve and surface curvature. And the proximity size function can be used for creating the surface mesh based on the number of cells per gap specified. We can improve surface mesh quality limit.

In Describe geometry section, we must specify the type of geometry having solid or fluid domains consisting of voids or without voids. If volume extraction has done in space claim, then cap opening is not required in meshing. Fluid-fluid boundary types from wall to internal can be enabled if flow is allowed to pass through this interface. Share topology can be applied if it’s not created in space claim, this tool shares the faces of one body with another in a complex geometry with multiple body. This share of faces, makes the body as conformal model, therefore making the model compatible with the Fluent solver.

In update boundary, boundary conditions for the cell zones and labels can be specified. In add boundary conditions, there are four different boundary conditions to specify.

Smooth transition specifies the transition ratio as the ratio of last prism cell height to the size of first non-boundary layer cell. Smooth growth rate and prism cell to volume change at outer boundary layer can be observed. Whereas no control of first layer height and inconsistent total height is created in this type of boundary layer.

Aspect-ratio is the ratio of the first prism cell height to the size of the base prism. It is useful for variable mesh size on boundaries with consistent growth rate. Whereas no control of first layer height and inconsistent total height gets created in this type of boundary layer.

Uniform type boundary layer creates same first layer height and consistent total height throughout the boundary cells. But it can lead to problems with high and low aspect ratio calls.

In last-ratio boundary layer, all cells have same first layer height and same ratio of last prism. It can give smooth transition from prism to cell at boundary layer edge, but growth rate varies to satisfy other inputs.

Fluent can create four different structures of volumetric meshes. Tetrahedral mesh creates mesh of tetrahedral shapes. Hexacore meshing generates cartesian cells insides the core of the domain and tetrahedral cells close to the boundaries This type of meshing enables efficient cell size transition from boundary to interior of the domain. It can handle complex geometries with large internal regions.

Polyhedral meshes contains polyhedral cells which can provide lower cell count than the tetrahedral mesh. So, the solution can converge generally faster using polyhedral mesh, thus saving the computational expense. The prerequisites for generating polyhedral mesh are triangular surface mesh with better orthogonal quality and the aspect ratio should be less than 50. The other type of volumetric mesh is Poly-hexacore meshes containing the combination of polyhedral and hexacore cells. So, it can be used for complex geometries without significant rise in computational duration and expense.

"The grid independence test has been done at various cell count and at node of 2.46 million cells the simulation has been conducted. As beyond this grid cell, the flow distribution results are approximately same." Once the meshing is complete, the skewness reported in the console window is to be checked. Generally, the maximum skewness for the surface mesh is desired to be less than 0.7 for getting mesh of higher quality. Skewness is a measure of inaccuracy in mesh structure, so it should be least.

$$\{\text{Minimum Orthogonal quality} = 1 - \text{skewness}\} \tag{7}$$

After the completion of volumetric mesh, the console window will show the minimum orthogonal quality of the mesh. The minimum orthogonal quality for a volumetric mesh should be 0.1, for better quality mesh.

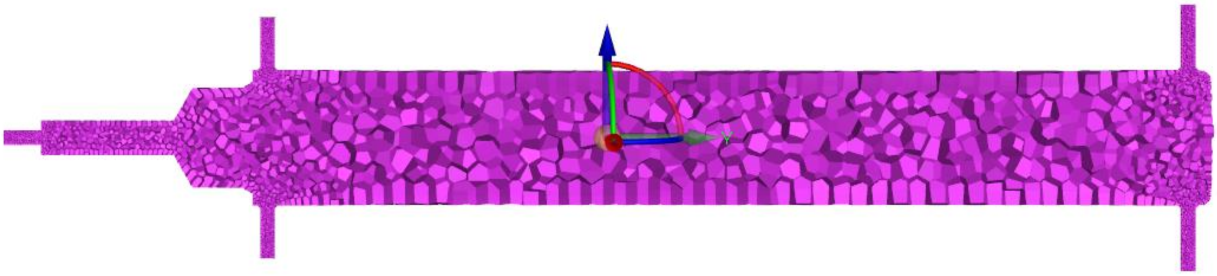

Fig.17 Polyhedral Mesh showing cut edge with cell layer

4.5.1 Meshing Details

Total number of nodes	2463686
Number of edges	10268
Number of faces	3528150
Face size	0.25
Orthogonal quality	0.1
Maximum Aspect ratio	3.81 e+02
Skewness	0.68
Minimum cell size	0.2 mm
Boundary layer type	Last ratio
Number of boundary layer	5
First height of boundary layer	0.05 mm
Transition ratio	0.272

Table 1. Meshing details

4.6. Methodologies used in Ansys- Fluent solver

The methodology of Fluent solver consists of three basic steps. Setup, pre-processing, and post processing. The numerical method development for end winding cooling follows the simulation approach as, initially the oil flow simulation in the rotor shaft is performed using the pseudo transient method till the flow of oil gets developed in the rotor shaft. The pseudo transient approach is used initially for shaft simulation using moving reference frame (MRF) method. In MRF method the outer domain of the body along is not rotating but the effect of motion is observed inside the body. Thus, saving the computational expense in the initial stage of simulation.

The pseudo transient method is a part of steady state method in which the time scale factor is provided which gets multiplied with the relaxation factor, thus can increase the speed of simulation. The relaxation factor is responsible for computing the residual of continuity, x, y and z momentum equation for every iteration solved.

Initially in the Fluent solver we specify a general setting in the setup tab in which the solver type provides the solution method for computing the solution which contains pressure based or density-based Navier stokes solution algorithm. The velocity formulation can be specified as absolute or relative.

Gravity can be enabled, and gravitational acceleration is specified based on the coordinate's axis of the model. And the 2D space options like planar, axisymmetric, and axisymmetric swirl can be used based on the model requirement. At high rotational speed, gravity is not considered because the centrifugal acceleration is much larger than the gravity. Energy equation is recommended to be disabled for performing iso-thermal simulations, which helps in running stable simulation.

Numerical description-Assumption:

1. The two phases simulation is intended to investigate the two-phase flow (Air/Oil) inside the shaft and associated heat transfer is not modelled
2. Surface tension is not considered as it is negligible due to high weber number.
3. The gravity effect is ignored in the simulation. Later it will be included to evaluate the impact.
4. The oil property is defined at constant temperature
5. The air property is taken from Fluent material data base.

4.6.1 Preprocessing Settings:

The preprocessing settings used in Ansys Fluent are as follows:

- Steady-state modeling (Pseudo-transient method)
- Primary phase: Air, Secondary phase: Oil
- INLET: 100% Oil flow + 0% Air flow
- OUTLET: Opening condition + 0% Oil reverse flow
- Backflow direction from neighboring cell at OUTLET
- Turbulence Model: SST K-ω (2 eqn.)
- Full domain filled with **air (or Oil) at the start**, relative to cell zone initialization
- SRF (Single Reference Frame): Frame motion model is used
- Gravity is not activated due to high rotational speed
- No surface tension effect due to high weber number flow

4.6.2 Recommendation- Defining Phases:

In general, primary, and secondary phases can be defined arbitrarily. For ease of the problem setup, give names for the phases as only the secondary phase(s) volume fraction(s) is (are) solved, it's (their) initial volume fraction can be patched in part of the domain. "Primary" phase volume fraction is deduced from secondary phase(s) volume fraction(s)

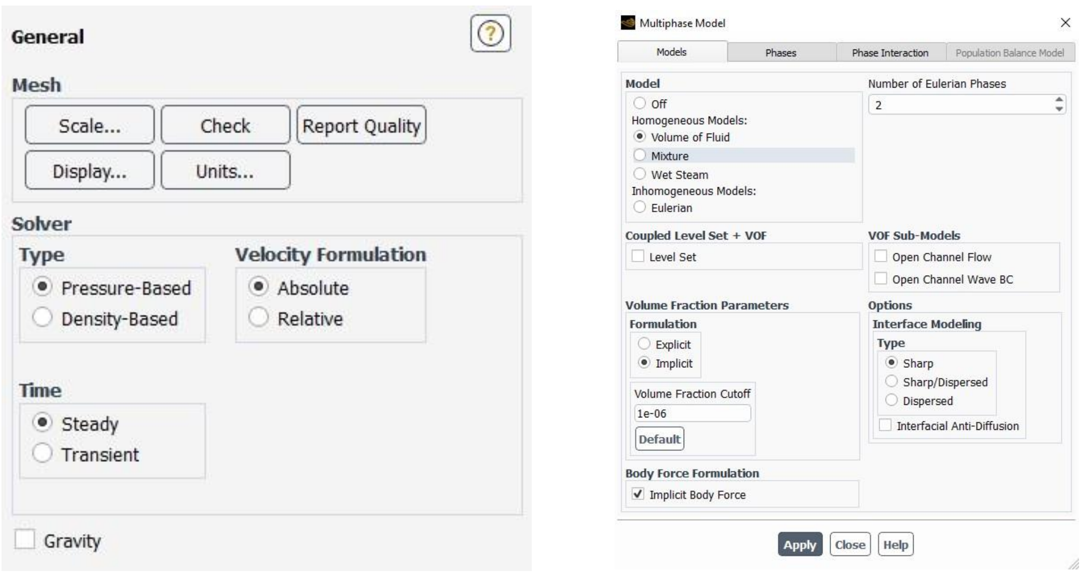

Fig.18 (a) General setting (b) Multiphase model setting

Volume fraction cutoff specifies the lower limit of volume fraction, below which the value is considered as zero. The default value is 1e-6. The implicit body force increases the solution stability and enhances the convergence for high rotational flow with large body forces.

In VOF model, the interference modelling provides some interface tracking scheme. Sharp scheme is recommended for electric motor when distinct interface is between the phases. Dispersed scheme is used when secondary phase is dispersed in primary phase. Sharp/dispersed is used when secondary phase is present in both separated and dispersed state in domains. The interfacial anti-diffusion suppresses the chance of numerical diffusion which may occur with coarse meshes, skewed mesh, high aspect ratio cells or large jump in cell volume near the interface, but it can also affect the solution convergence at times.
Along with the interface of two phases, the effect of surface tension is also considered in VOF model. The surface tension generates due to the attractive force between the molecules in a fluid. Reynold number is to be evaluated for determining the significance of surface tension. For Re<<1, Capillary number is considered and for Re>>1, weber number is considered. The surface tension force can be neglected for most high-speed applications, due to its high inertial effects the Weber number is very large.

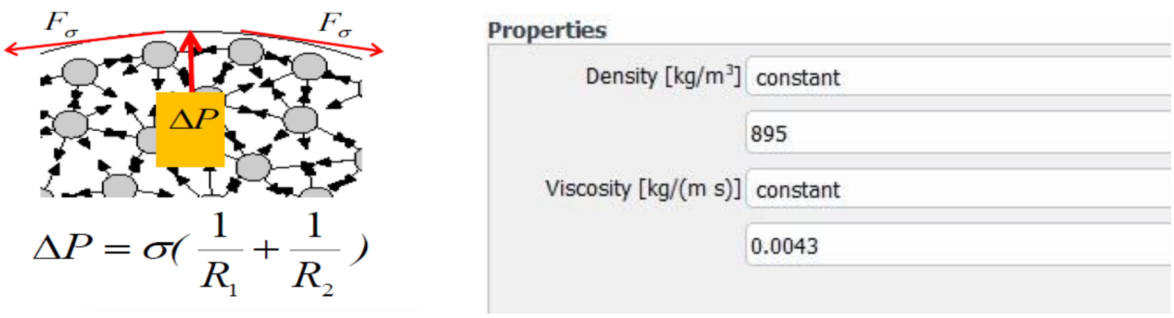

Fig.19 (a) Image describing surface tension (b) Image showing the material properties of oil

In viscous model, SST k-omega model is used which predicts better near the wall surface. Enabling the energy equation will formulate the temperature equation and the thermal properties of materials are specified. Surface tension is not considered in this problem as it is a high weber number flow, due to high inertial effect.

Compressive VOF scheme (with Flux Averaged method) is recommended over Geo-Reconstruct scheme for applications with high-speed rotating zones due to higher robustness and higher accuracy as compared to Geo-reconstruct scheme when operating at larger time step sizes (C>=1).
In the physics tab, material properties are specified. The phase of interest is suggested to specify as secondary phase. If air is specified as ideal gas, it should be specified as the primary phase for better numerical handling. For many high-speed simulations, it is suggested to specify liquid as compressible and air as ideal gas because the oil-air compressibility effect is important.

In cell zone condition, zones are selected for specifying the mesh motion. Rotational velocity, tangential velocity, rotation-axis direction, and origin coordinates are specified for cell zones. Mesh motion is given for (SMM) sliding mesh motion condition, where motion of the objects is captured. Whereas frame motion uses MRF method in which object motion is not captured. When using mesh motion, mesh interfaces are created for avoiding the mesh rupture due to wall movement.

4.6.3 Boundary Condition:

Inlet Section	**Outlet Section**
Mass flow inlet (kg/s)	Pressure outlet

Table 2 Boundary Condition used in the inlet and outlet section

Boundary conditions for inlet zones are set as “mass flow rate”. Since in our case, the input parameter is flow rate. This boundary condition is set for both oil shaft inlet and stator shower inlet zones. The reference frame is set as absolute to specify the exact value. The initial gauge pressure is set as zero as a atmospheric pressure. The direction specification method is set as “normal to boundary”. Specifying the flow to enter the shaft normal to the inlet boundary. Keeping the default turbulence specification method with intensity percentage as 5 and viscosity ratio as 10.

The outlet boundary conditions are given for the end space oil outlet as “Pressure outlet”. The pressure specification method is selected gauge pressure specifying as an atmospheric pressure. The backflow direction specification method is “from neighboring cell”. This specifies that the outlet flow will be based on the direction normal to the neighboring cell. It is critical for accurate air entrainment modelling in highly swirling flow. The backflow pressure specification is selected as “total pressure” and with a backflow oil fraction as zero.

The mesh interfaces are created when changing moving reference frame to sliding mesh motion. The internal are those zones where fluid is supposed to flow across. The wall contains those zones where fluid cannot flow across and can behave as a wall.

Thermal boundary conditions are used when energy equation is enabled. The backflow total temperature is used to set the total temperature of the inflow stream that flows in the reverse direction.

4.6.4 **Pressure-velocity coupling**

Pressure velocity coupling derives a condition for pressure by correcting the governing equation and allows to solve the flow problem in either segregated or coupled manner. The five pressure-velocity coupling algorithms are: Simple, Simple, PISO, Coupled and Fractional step.

Simple algorithms enforce the continuity equation to obtain the pressure field using the relationship between pressure and velocity corrections. Simple algorithm (Simple Implicit Method for Pressure Linked Equation) substitutes the flux correction equations to obtain a discrete continuity equation for the pressure correction in the cell.

SIMPLEC (Simple Implicit Method for Pressure Linked Equation- Consistent) is a variant of Simple algorithm, which is default for transient simulations. In this a modified face flux correction is used to accelerate convergence in problems where pressure -velocity coupling is involved.

PISO (Pressure-Implicit with Splitting of Operators) is a pressure velocity coupling scheme, which stands for pressure-implicit with splitting operators. It is based on the higher degree of the approximate relation between the correction of pressure and velocity. It can overcome the limitation of SIMPLE AND Simplec as the new velocity and corresponding fluxes satisfies the momentum balance after the pressure correction equation is solved. As a result, the calculation must be repeated until the balance is satisfied. To improve the efficiency of this calculation, PISO algorithm performs two additional corrections: neighbor correction and skewness correction. Use of presto is highly recommended for rotational flows with high swirl.

Coupled algorithm solves the momentum and pressure-based continuity equations together, thus obtain a robust and efficient single-phase implementation for steady state flows, with superior performance compared to the segregated solution scheme. For transient flows, using the coupled algorithm is necessary when the quality of the mesh is poor or if large time steps are used. The pressure based coupled algorithm differs from simple-type segregated algorithm, as it solves the momentum equation and pressure correction equation separately, which results in slow convergence. By default, coupled solver is selected with Pseudo-transient method.

Skewness Correction reduces the convergence difficulty associated with highly distorted meshes. The approximate relationship between the correction mass flux at cell face and the difference of pressure correction at the adjacent cells is very rough. The PISO skewness correction is used to obtain a solution on highly skewed mesh in approximately the same number of iterations as required for a more orthogonal mesh.

The FSM (Fractional step method) is used in Ansys Fluent as a velocity coupling scheme in a non-iterative time advancement (NITA) algorithm. In this the momentum equations are decoupled from the continuity equation using a mathematical technique called approximate factorization.

4.6.5 Solution Methods

In pseudo-transient case, coupled solver is selected by default. It solves the momentum and pressure based could equation together and gives robust solution. Default compressive scheme is used for volume fraction spatial discretization. Second order upwind for spatial discretization of momentum, turbulent kinetic energy and specific dissipate rate. Least square cell-based formulation is used in gradient discretization. For pressure discretization, PRESTO (PREssure STaggering Option) and modified Body force weighted can be used. PRESTO scheme is more generalized and sensitive on mesh and time step size. PRESTO pressure discretization should be used for high rotating case with iterative solver.

Whereas, modified BFW (Body Force Weighted) has better robustness and convergence with NITA solver. It has few limitations with highly viscous and rotating flows. Warped face gradient correction and high order term relaxation is used.

In transient method, PISO pressure-velocity coupling should be used for faster solution convergence per time step with the iterative solver than SIMPLEC.

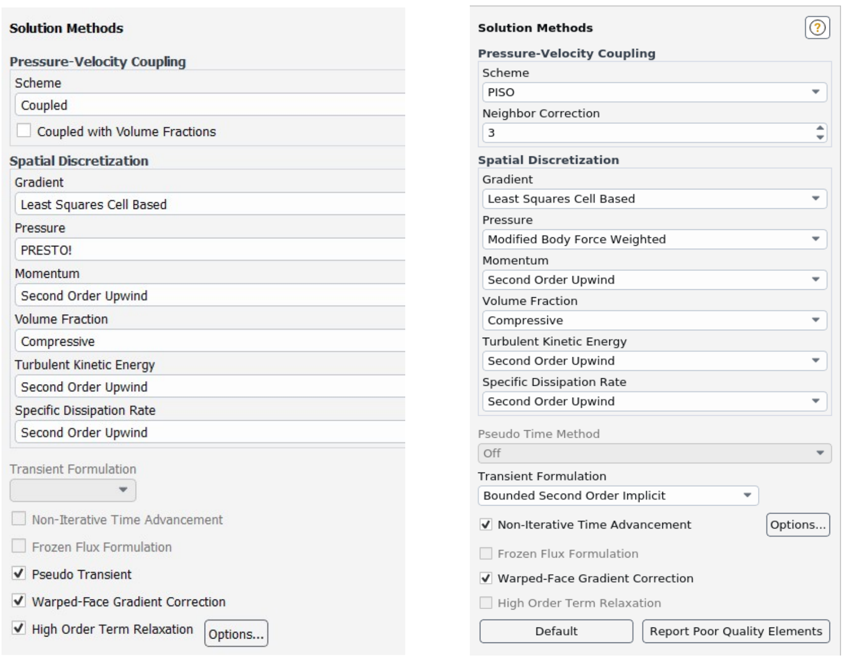

Fig.20 (a) Solution methods for Pseudo-transient method (b) For transient method

Whereas, modified BFW has better robustness and convergence with NITA solver. It has few limitations with highly viscous and rotating flows. Warped face gradient correction and high order term relaxation is used. In transient method, PISO pressure-velocity coupling should be used for faster solution convergence per time step with the iterative solver than SIMPLEC.

4.6.6 Automatic Mesh Adaption technique

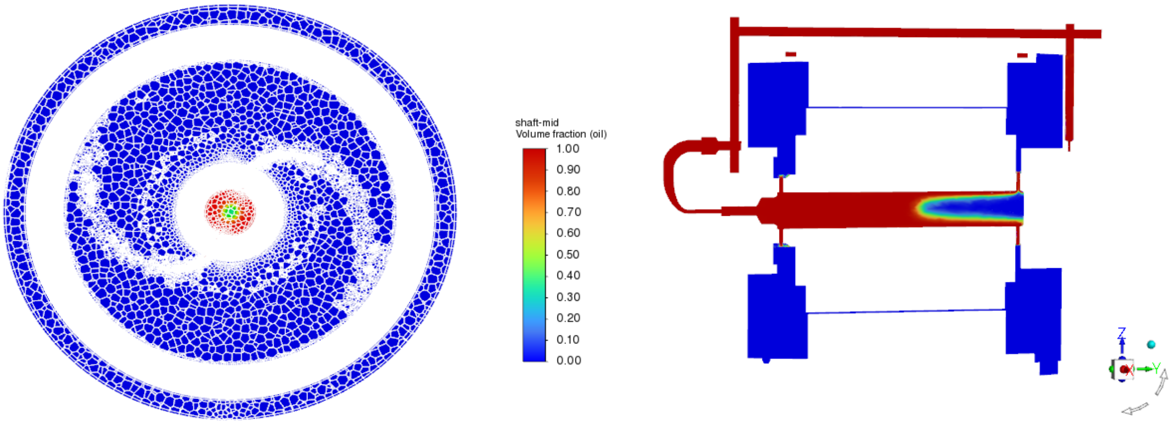

Fig.21 (a) Mesh adaption contour in the end-windings (b)Mid-plane contour of shaft and end-windings

Methodology used in PUMA

1. Select Automatic Mesh adaption in Solution tab.
2. Under Predefined Criteria and select VOF and minimum cell length(L) for mesh refinement.
3. Cell Registers defines the criteria for VOF refinement and coarsening based on oil fraction.
4. General mesh adaption defines zone of mesh adaption, maximum refinement level and minimum orthogonal quality.
5. Selecting automatic mesh adaption, creates named expression for vof_refinement which defines 3 following criteria: oil fraction of Vof refinement, Minimum cell volume and Maximum cell refinement level.

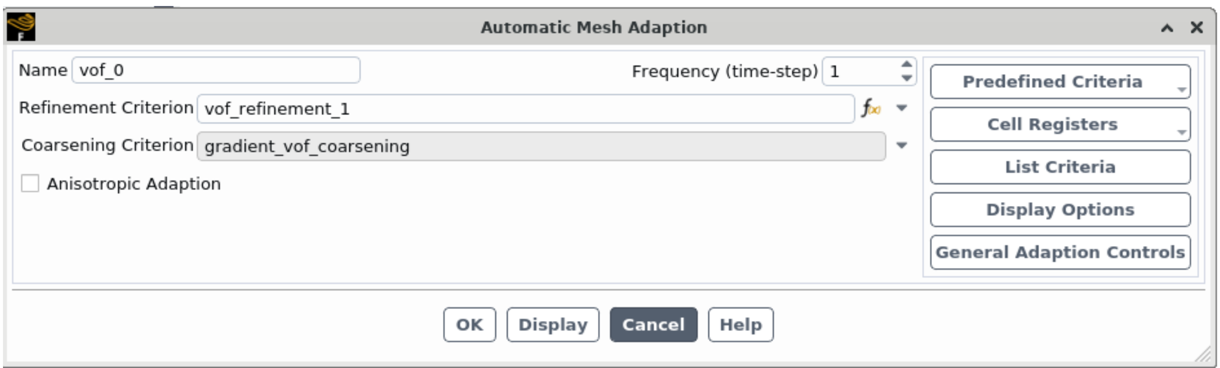

Fig.22 Image showing the settings used PUMA technique

4.6.7 <u>Methodologies used for Invoking Hybrid Nita:</u>

In the solution method, using PISO scheme in transient simulation, non-iterative time advancement option is enabled. Enabling the Hybrid Nita option, we get two options:

- <u>Aggressive</u>: For incompressible flow situation with low viscosity and low surface tension, aggressive Nita scheme can give more speed-up. It solves 2 outer iteration per time step.
- <u>Conservative</u>: Mainly used for surface tension dominated flow and gives a better stability. It solves 3 outer iteration per time step.

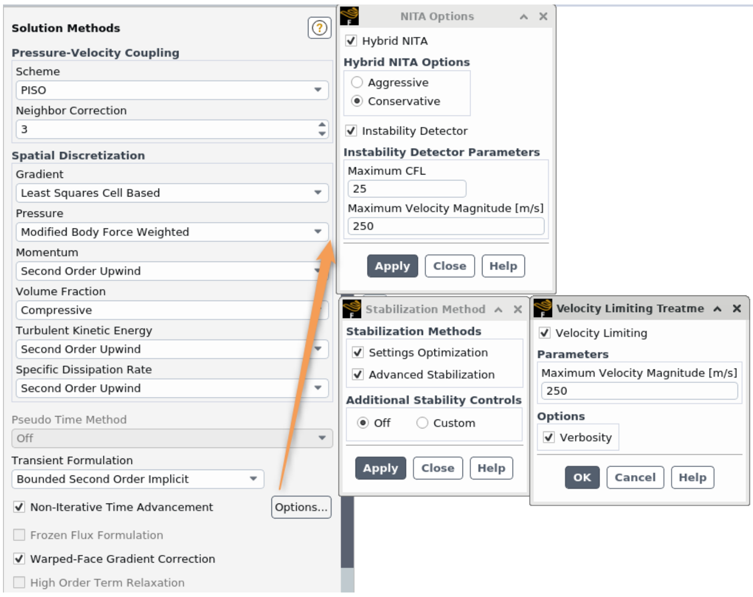

Fig.23 Settings used for invoking Hybrid NITA

Verbosity in velocity limiting treatment shows that how many cells have got restricted when velocity limiting is applied. It is advised to save the case and data file before applying NITA scheme, because reverting to the previous state cannot be supported in Fluent.

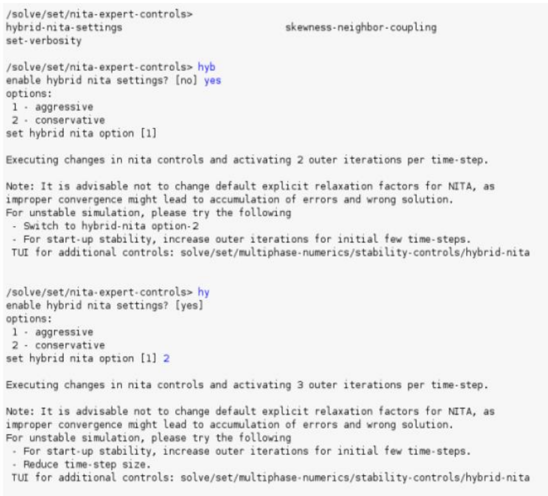

```
/solve/set/nita-expert-controls>
hybrid-nita-settings                    skewness-neighbor-coupling
set-verbosity

/solve/set/nita-expert-controls> hyb
enable hybrid nita settings? [no] yes
options:
 1 - aggressive
 2 - conservative
set hybrid nita option [1]

Executing changes in nita controls and activating 2 outer iterations per time-step.

Note: It is advisable not to change default explicit relaxation factors for NITA, as
improper convergence might lead to accumulation of errors and wrong solution.
For unstable simulation, please try the following
 - Switch to hybrid-nita option-2
 - For start-up stability, increase outer iterations for initial few time-steps.
 TUI for additional controls: solve/set/multiphase-numerics/stability-controls/hybrid-nita


/solve/set/nita-expert-controls> hy
enable hybrid nita settings? [yes]
options:
 1 - aggressive
 2 - conservative
set hybrid nita option [1] 2

Executing changes in nita controls and activating 3 outer iterations per time-step.

Note: It is advisable not to change default explicit relaxation factors for NITA, as
improper convergence might lead to accumulation of errors and wrong solution.
For unstable simulation, please try the following
 - For start-up stability, increase outer iterations for initial few time-steps.
 - Reduce time-step size.
 TUI for additional controls: solve/set/multiphase-numerics/stability-controls/hybrid-nita
```

Fig.24 TUI command for enabling Hybrid NITA

Effect of instability detector

Based on our flow simulation, we use conservative approach for better results with 3 outer iterations per time-step. Instability detector option is to be enabled, that can detect the unstable event based on CFL criteria or velocity limit. Once it gets detected, it increases the outer iteration to 5 for hybrid Nita during the current time-step to improve the convergence behavior. It continues this until the courant number or velocity falls below the limit. It is recommended to apply the Nita settings after the stabilization method.

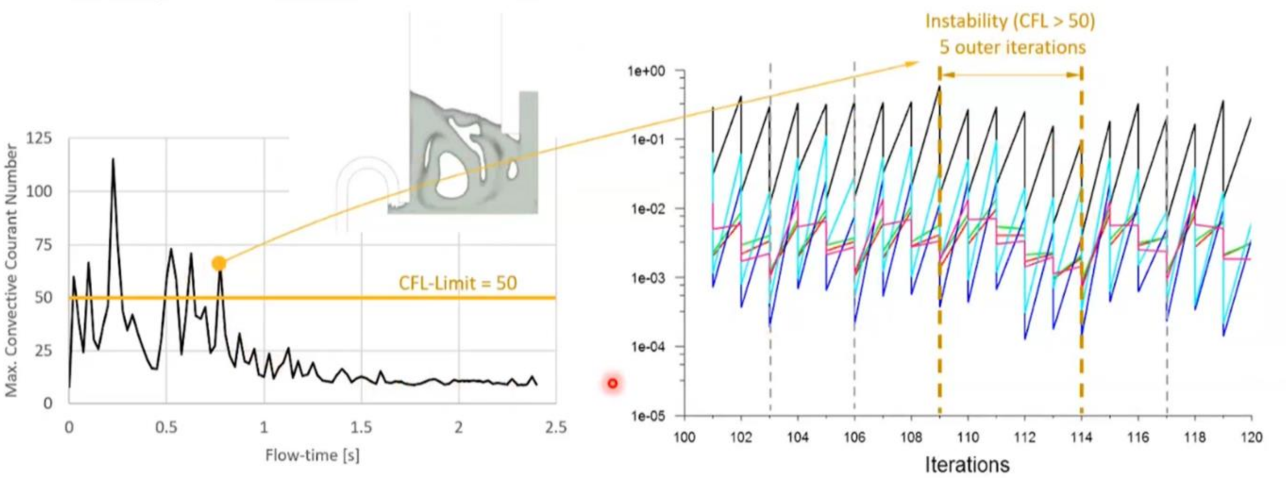

Fig.25 Image showing the effect of instability Detector [Courtesy: Ansys]

4.6.8 Methodology used in Conjugate Heat Transfer (CHT) Modelling:

In mixed-time step coupling, a guess temperature of rotor & windings is taken in fluid extracted domains. This initial guessed reference temperature is guessed based on their threshold temperature bearing limit of the material. This result is to be used in fluid simulation and the HTC value is extracted. Besides, heat flux is given in water jacket case and the HTC value is extracted. Both the HTC value will be used as input parameter for solid simulation & temperature value is extracted. This process is continued till we get stable results.

Requirements from CHT modelling: Steady state temperature distribution, Transient evolution of temperature field, Cyclic/ Pseudo cyclic state temperature distribution.

The fluid extracted domains has low thermal inertia. Whereas the solid domains have higher thermal inertia. So, the time step size required to simulate the fluid domains will be smaller than solid domain. So, both the domains will be meshed and simulated separately. Combining both the domains for simulation can cause large mesh count which can increase the computational time and expense. Also due to the mesh motion in the multiple zones, the chance of divergence will increase.

Assume a wall temperature in the boundary of the fluid domain. Removing all the solid domains & simulating only fluid domains. Then applying the HTC from fluid to the solid. Using HTC value, simulating the solid domain & getting the reference temperature.

The desired expectation is getting the temperature distribution of solid surfaces and later the thermal stresses and the life of the components.

Time- averaged heat flux profile is extracted on the fluid side & apply on the solid side. Once the solid gets the heat flux, the solid temperature changes, then the updated wall temperature is given to the solid side. The iteration is to be continued till we get the converged results.

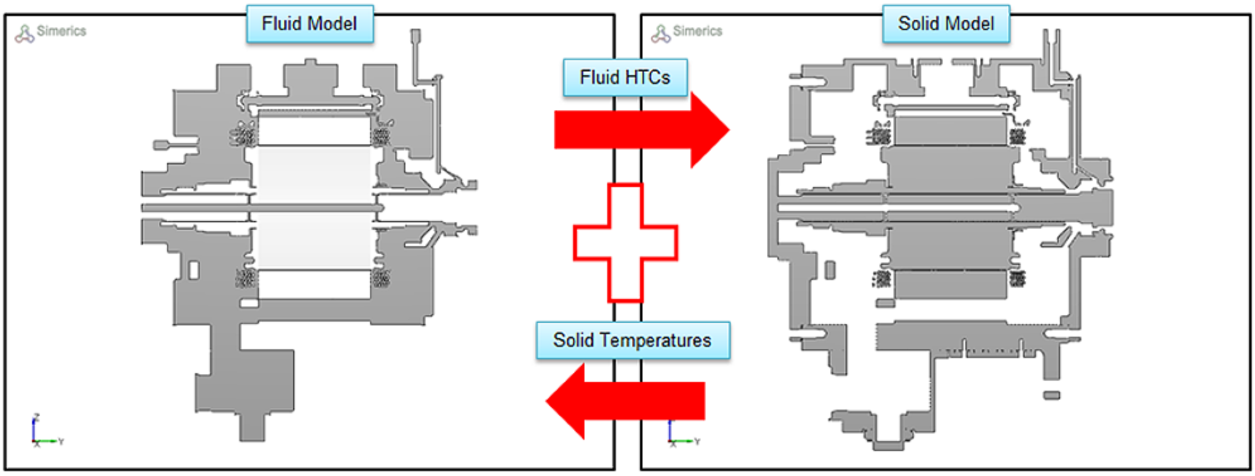

Fig.26 Picture showing the mixed-timescale coupling approach, Srinivasan et.al [1]

Loosely coupled approach:

Loosely coupled approach is applied on the transient case, with both solid and fluid domains are combined. In run calculations, specify solid time step size using fixed type and user-specified method. Using instantaneous Implicit coupling method, the coupling frequency can be specified. The solid time step size can be computed as the coupling frequency times of the fluid time step size. At coupling frequency of 360, the solid time step size is to be the time required to complete 1 rotation of the shaft. Since, the time required to complete 1 degree of rotation is considered as the time step size for fluid simulation.

Explicit CHT Modelling Method:

The other coupling method is time-averaged explicit, in which the solid is solved at all time step with the fluids. Used for load-cycle simulation, for capturing temperature rise and fall. We can use this coupling scheme on those walls where jet is striking. In this method, the number of time steps per coupling iterations is specified, which provides the coupling frequency after which the mapping between the two domains should be performed. Enabling moving average will average the specified number of previous iteration results and map the average results to the other domain.
Using the moving average scheme, we can increase the coupling between solid and the fluid without increasing the simulation time.

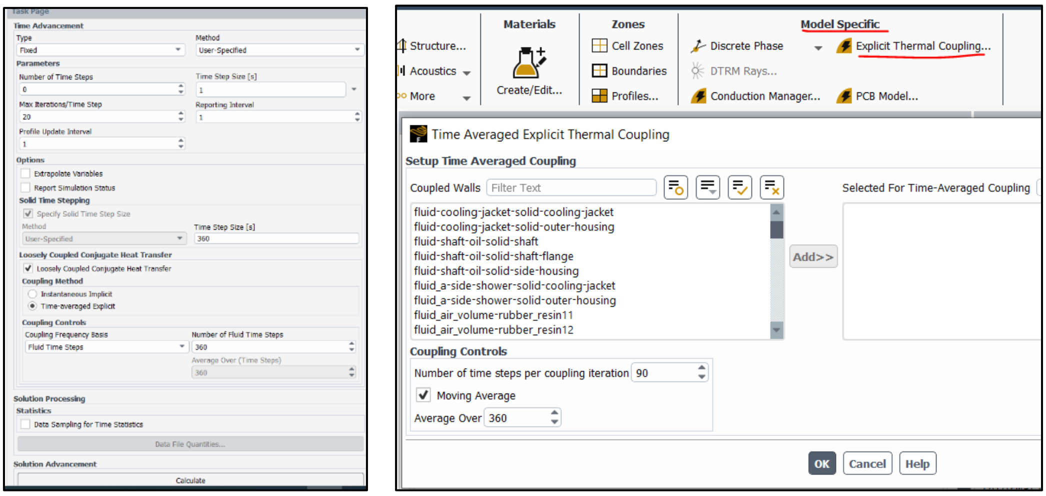

Fig.27 Methodology used in (a) loosely coupled coupling (b) Explicit Thermal coupling

4.6.9 Convergence Criterion & Monitored Variables

The convergence is reached when changes from one iteration to the other iteration in the solution variables are negligible. The residual plots help in monitoring the trend of convergence. With the stability in convergence plot, the overall property conservation is achieved with least imbalance of the property. The convergence also shows that the quantity of interest has reached the steady values, as monitor points track the overall area of interest.

The converged solution should satisfy the following:

1. Residuals at least < 10^{-3} for all equations.
2. Mass conversation checks should be satisfied.
3. Plausibility of contour plots and flow distribution should be checked from intermediate files.

Residuals- convergence checks:

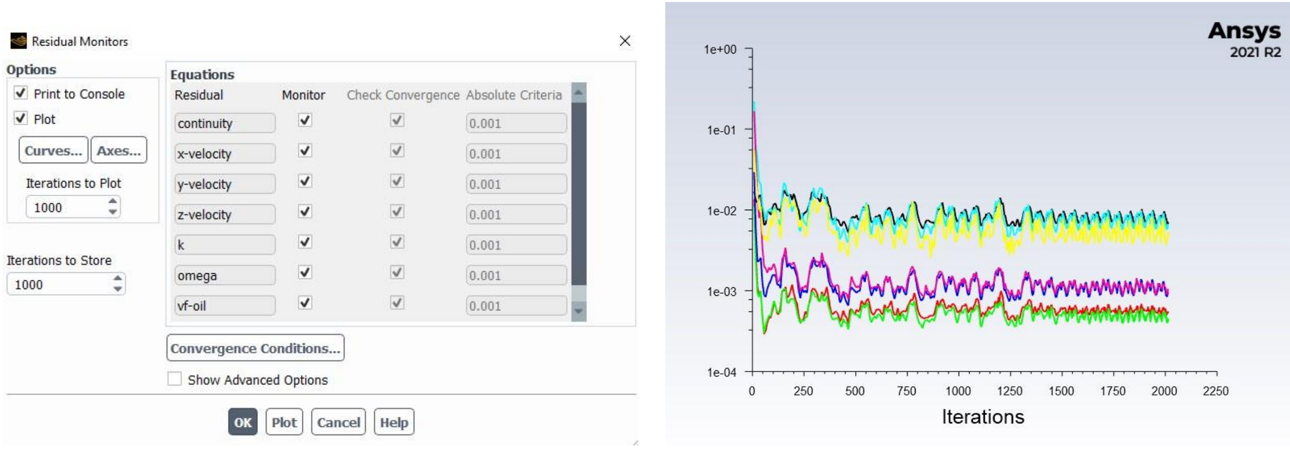

Fig.28 (a) Image showing Convergence criteria (b) Representation of residual plots

Mass- conservation checks

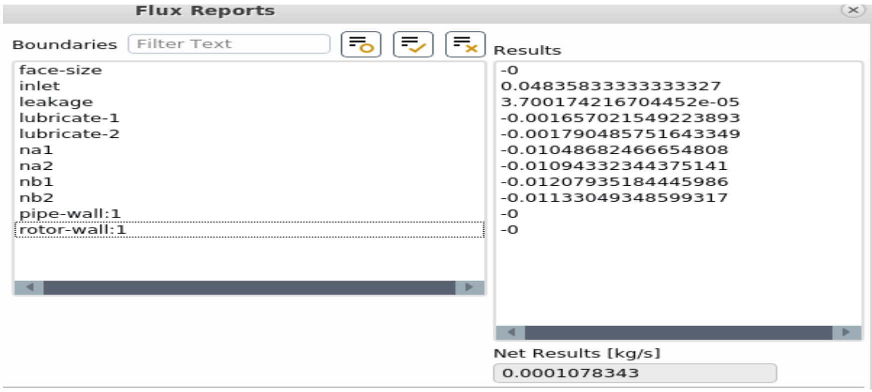

Fig.29 Flux report of mass conservation check

The acceptance criteria of mass imbalance are less than 5 %. Below this percentage imbalance, the solution is assumed to be converged based on continuity equation. In the above figure, the net sum of all the mass flux in the flux report is 0.2%, thus can be said as a converged equation.

Chapter 5

Validation of the Numerical model

Sharma et al. has developed a CFD methodology to analyze the flow split-up between the two rows of nozzle in which Opti slang tool is used for postprocessing of design sensitivity analysis. The geometry used in this paper, Sharma et.al [13] is replicated and simulation is conducted using Ansys Fluent software to verify the oil distribution results.

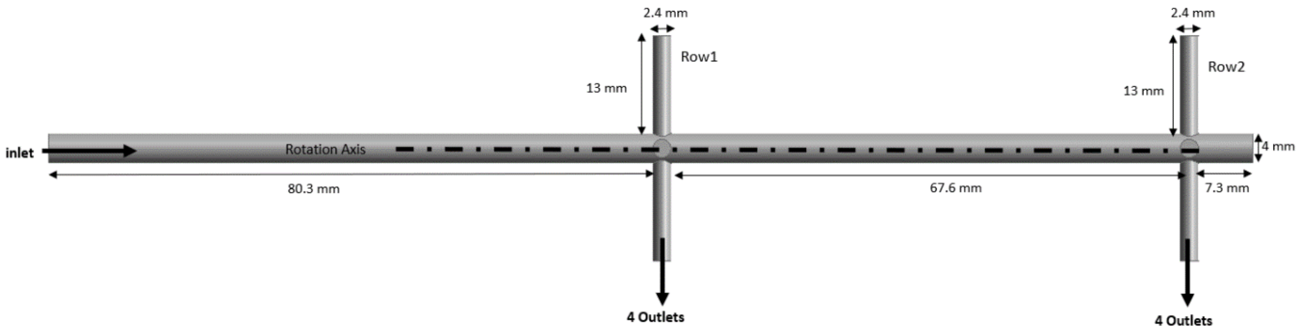

Fig 30 (a) Schematic diagram of the 3D hollow rotating shaft, Sharma et.al [13]

In order to validate the results of flow distribution between two rows of nozzles of the rotating shaft at different mass flow rate and rpm, same geometrical dimensions are used keeping all the same mass flow rate and rotational velocity as used in Sharma et.al.[13]. The results are validated with the Fluent software used throughout in this simulation study.

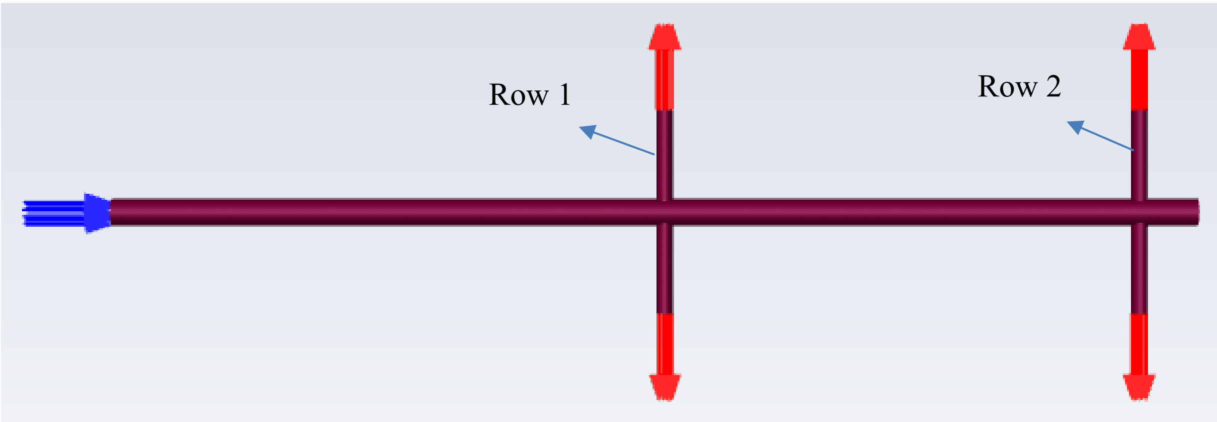

Fig.31 Image of hollow shaft with nozzles showing inflow and outflow of oil in Ansys fluent

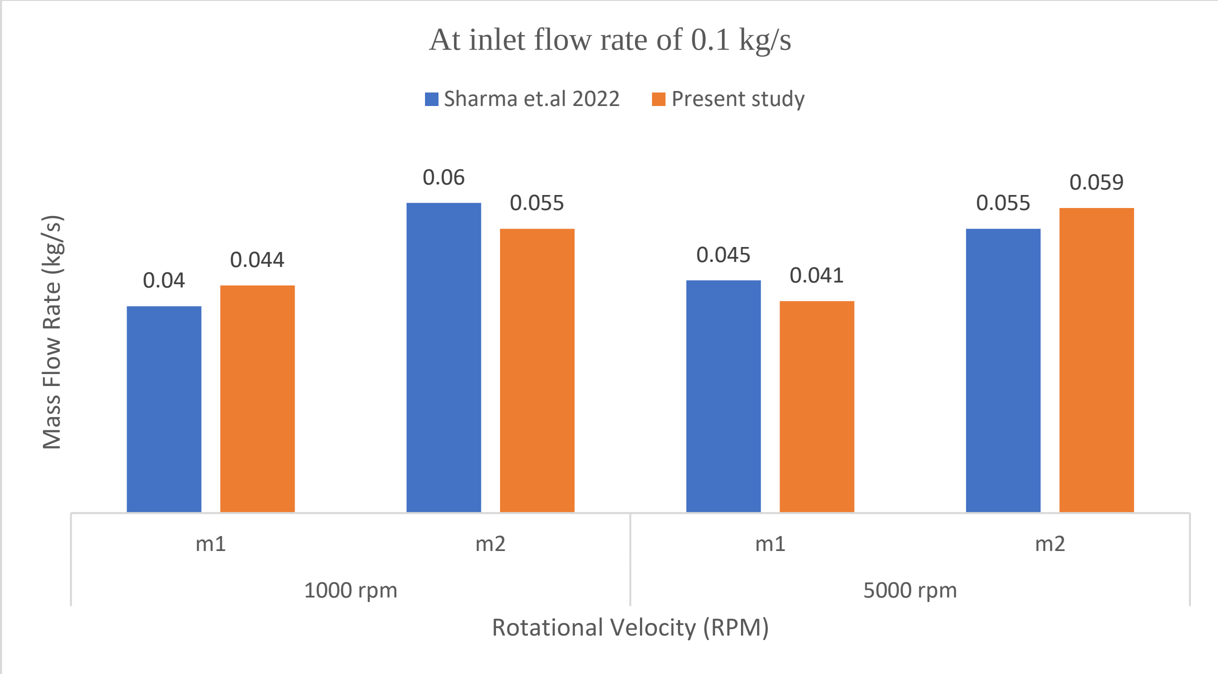

Fig.32 Graph showing the mass flow distribution at 0.1kg/s & 0.04 kg/s of both the study at their respective rpm

5.1 Observations from the validation results:

- The oil flow distributions of this study are compared with the results of Sharma et al [13].
- The deviation of mass flow results of present study with the reference paper[13] are less at 5000 rpm and more at 1000 rpm.
- The results obtained in this study has an overall percentage deviation of 7-10 % from the results of the reference paper Sharma et. al [13]. This deviation is because high mesh count of 3.2 million cell count simulated using high performance computing, whereas the cell count used in present study is 46988 cells.
- The mesh quality is the factor of this much deviation, but the trend of flow rate is same. With this validation, further simulation results are discussed in this report.

Chapter: 6

Results and Discussion

Simulation results are discussed in three categories:

- Steady state shaft simulation
- Transient simulation for computing wetting area
- Results of mixed time scale coupling

6.1 Results of steady state shaft simulation

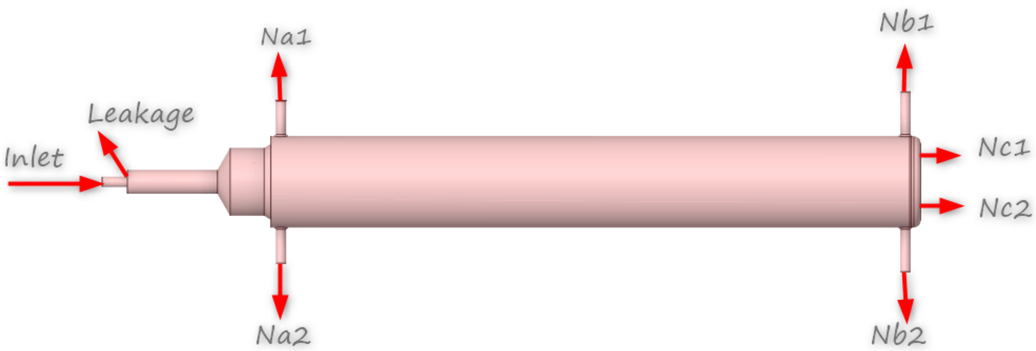

Fig.33 Schematic diagram of hollow shaft with nozzles

The mass flux report at different flow conditions is computed at inlet and all outlet nozzles. The 4 radial nozzles are (Na1,Na2, Nb1 and Nb2) for the oil splashing on the end-windings and the 2 axial nozzles (Nc1 and Nc2) are for the oil lubrication purpose. There is an air leakage zone near the inlet zone. The outflows from the rotor shaft are computed in such a way that the mass imbalance of the shaft would be under 2% of convergence limit.

Mass flow rate(kg/s) for different rpm and lpm																
Flow condition	**inlet**	**na1**	**%**	**na2**	**%**	**nb1**	**%**	**nb2**	**%**	**Nc 1**	**%**	**Nc 2**	**%**	**leakage**	**Net flowrate**	**%**
1lpm, 4rpm	0.07	0.02	23.28	0.02	27.18	0.02	22.00	0.02	27.18	2e-07	2e-04	3e-07	4e-04	0	2.49e-04	0.36%
0.7lpm, 3.55rpm	0.05	0.01	21.43	0.01	29.27	0.01	20.26	0.01	30.24	0	0	4e-06	8e-03	0	5.88e-04	1.22%
0.7lpm, 2.67rpm	0.05	0.01	21.16	0.01	26.37	0.01	21.15	0.01	28.27	3e-04	6e-01	3e-04	6e-01	0	8.81e-04	1.82%
0.7lpm, 1.78rpm	0.05	0.01	22.18	0.01	27.09	0.01	22.21	0.01	23.07	2e-03	3e+00	2e-03	4e+00	3e-05	6.91e-04	1.43%
0.7lpm, 1.11rpm	0.05	0.01	21.69	0.01	22.63	0.01	24.98	0.01	23.43	2e-03	3e+00	2e-03	4e+00	4e-05	3.38e-05	0.07%
0.7lpm, 0.22rpm	0.05	0.01	23.36	0.01	20.21	0.01	23.90	0.01	18.05	4e-03	8e+00	4e-03	8e+00	6e-05	5.41e-04	1.12%

Table 3 showing the flow distribution of oil between different nozzles at various flow parameters

The figure shows the data used in table 3 is presented below in a graphical format for simplication.

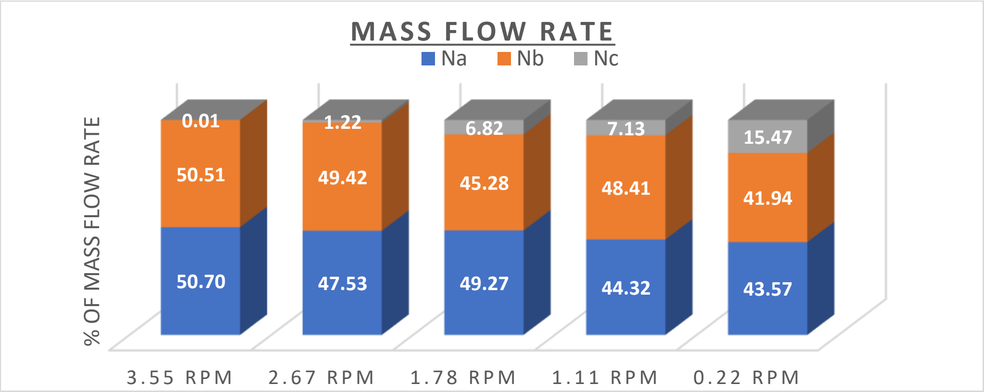

Fig. 34: Graph shows distribution between nozzles ar different RPM

[Note: The values of flow parameters are scaled value for the confidential reasons.]

Observation:

- Higher the rotational velocity, more will be the radial and tangential flow and lesser will be the axial flow of fluid.
- At lower rpm, the flow rate of a-side nozzle is more than that of b-side nozzle.
- With increase in rpm, the deviation of mass flow rate from a-side to b-side decreases as at high rotational speed of shaft, equal flow rate of oil is observed on both side of nozzle.
- With increase in rpm, the axial flow of oil decreases, as the centrifugal effect of shaft dominates on the flow velocity.
- At high rotational speed of rotor shaft, there will be no leakage through the shaft.

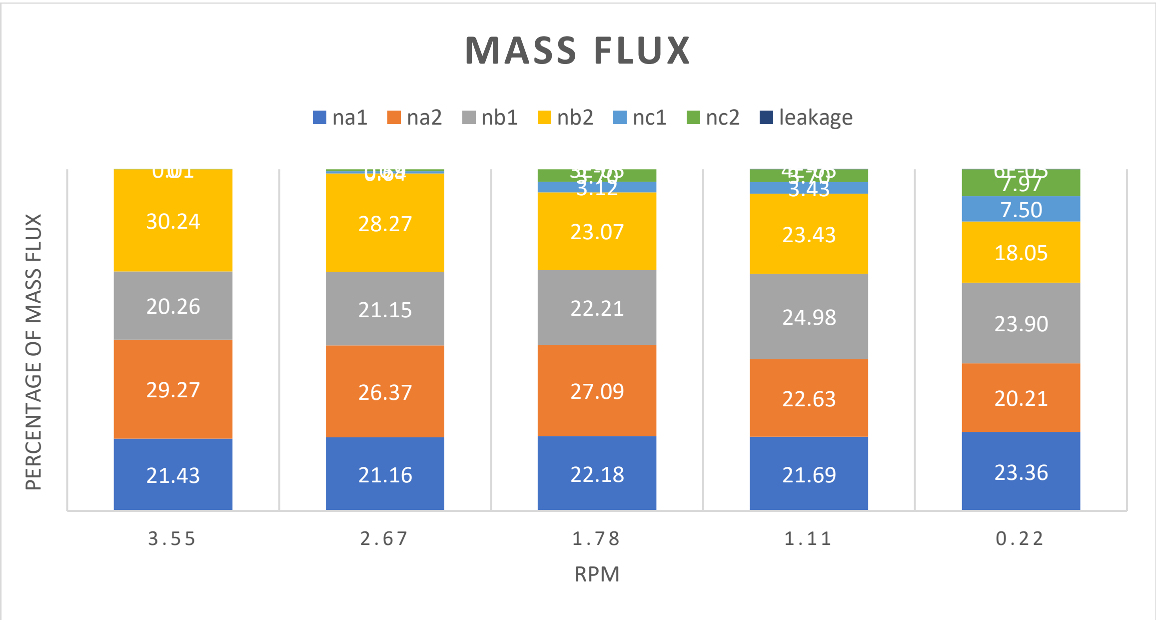

Fig.35 Graph shows the flow distribution presented in percentage of mass flux

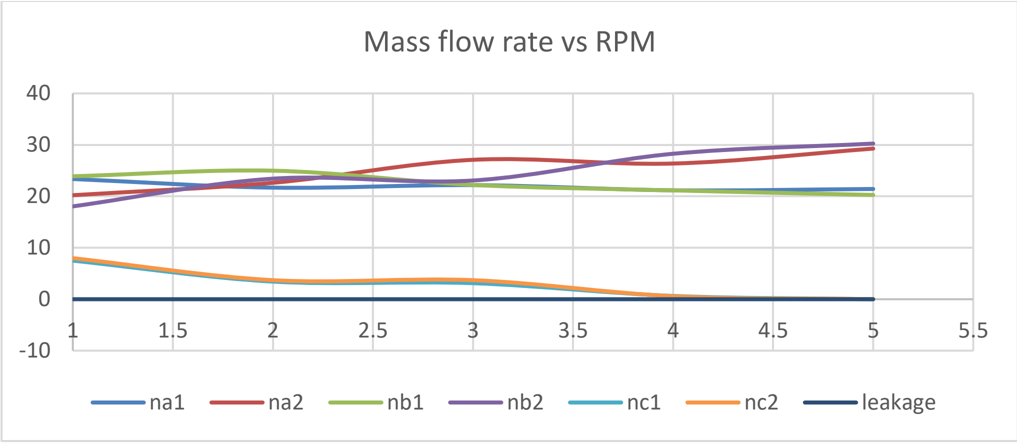

Fig. 36 Graph shows the trend of flow distribution in line graph representation

Comparing the mass flow rate with the gravity consideration

Mass flow rate at different rpm and lpm (Without Gravity)															
Flow condition	**inlet**	**na1**	**%**	**na2**	**%**	**nb1**	**%**	**nb2**	**%**	**nc 1**	**%**	**nc 2**	**%**	**leakage**	**Net flowrate**	**%**
0.7lpm, 2.67rpm	0.05	0.01	21.16	0.01	26.37	0.01	21.15	0.01	28.27	3e-4	0.6	3e-4	6e-1	0	8.81E-04	1.82%
0.7lpm, 1.78rpm	0.05	0.01	22.18	0.01	27.09	0.01	22.21	0.01	23.07	2e-3	3	2e-3	4	3E-05	-6.91E-04	1.43%

Mass flow rate at different rpm and lpm (With Gravity)																
Flow condition	**inlet**	**na**	**%**	**na2**	**%**	**nb1**	**%**	**nb2**	**%**	**nc 1**	**%**	**nc 2**	**%**	**leakage**	**Net flowrate**	**%**
0.7lpm, 2.67rpm	0.05	0.01	20.82	0.014	29.34	0.01	21.55	0.014	29.26	2e-05	3e-02	1e-05	2e-02	0	4.95e-04	1.02%
0.7lpm, 1.78rpm	0.05	0.01	23.78	0.013	26.26	0.01	24.63	0.012	24.08	2e-04	3e-01	1e-04	3e-01	3e-05	3.44e-04	0.71%

Table 4 showing the comparison of with and without gravity consideration

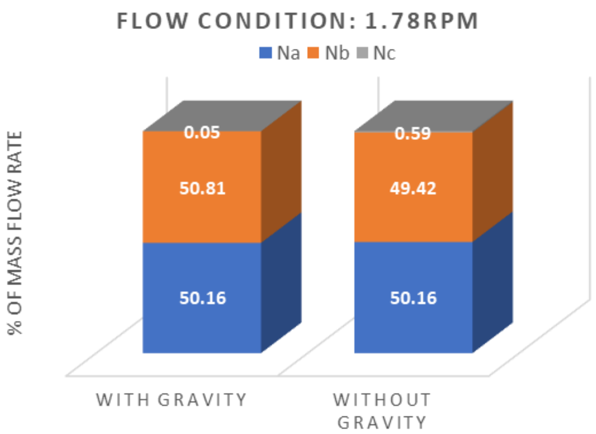

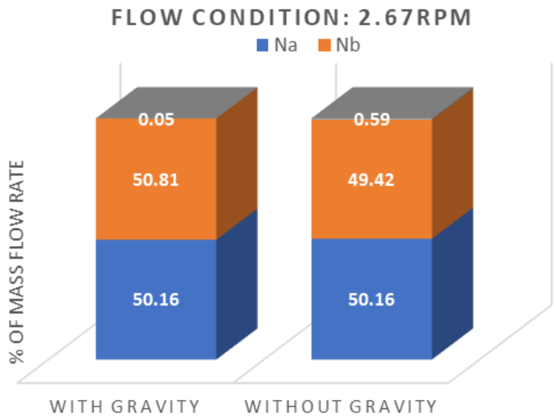

Fig. 37 Graphical representation of different flow condition with and without gravity consideration

Comparison of initialization state

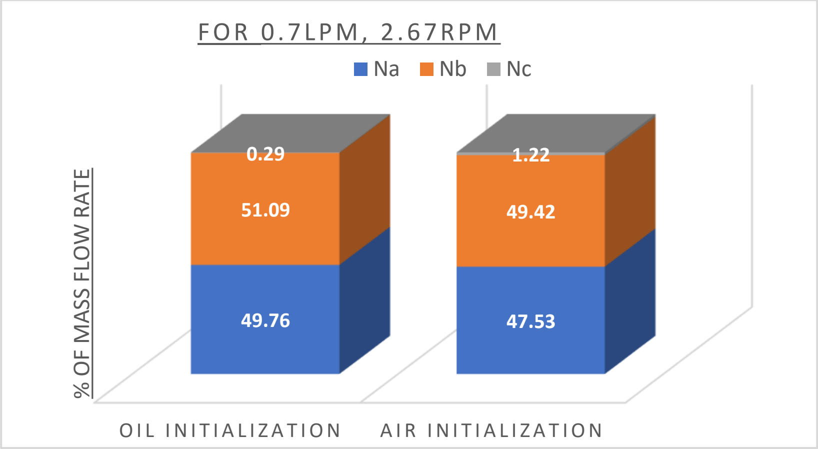

Fig. 38 The comparison of oil and air initialization state at certain flow parameter

At 12000 rpm, the mass flow rate for nozzle A and B has a variation of 1-2% from air initialization to oil initialization.

6.2 Results of transient simulation

The transient simulation is switched from pseudo-transient, as the mass imbalance reaches less than 5% in the shaft. The end-space region is patched with air, to compute the wetting area of the end-windings region. Oil wetting area on the windings are computed using a simplified model and computing the wetting percentage at the location of actual windings area, as shown in figure.

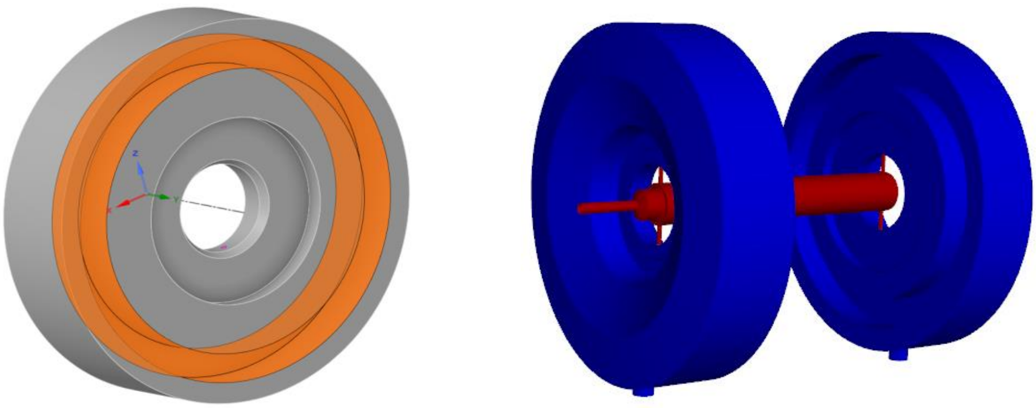

Fig.39 (a) Contour showing winding area on the end-space (b) Contour of end-windings with oil initialized shaft

The wetting percentage is computed based on the stability of wetting area with flow time. The stabilized value is noted as the final wetting percentage. Iso clip surface is generated on the winding area with more than 0.5 oil fraction, which is named as a wetting area. Expression is defined for wetting percentage as the percentage of wetting area with the total winding area. The computed value of A-side, B-side, and total wetting percentage, is mentioned.

Comparison of wetting percentage:

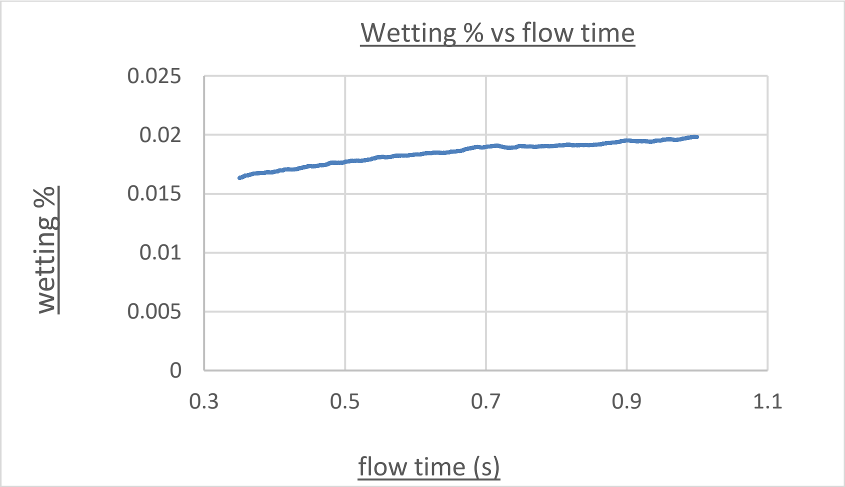

Fig.40 Graph showing the trend of wetting percentage with flow time

For 3 lpm & 1000rpm			
	Wetted area		
Condition	**A (%)**	**B (%)**	**total (%)**
Pseudo transient (20k it.)	23.62	16.63	20.48
Transient run (1sec)	29.81	25.14	27.71

Table 5. Showing the comparison of wetting percentage between transient and pseudo-transient scheme

The graph shows the plot of total wetting percentage with the flow time. And the comparison of wetting percentage between pseudo-transient (with 20,000 iteration) and transient simulation (with flow time 1sec), are shown in a table. This is concluded that we can get better wetting percentage when following the transient approach.

Comparison of end-space contour:

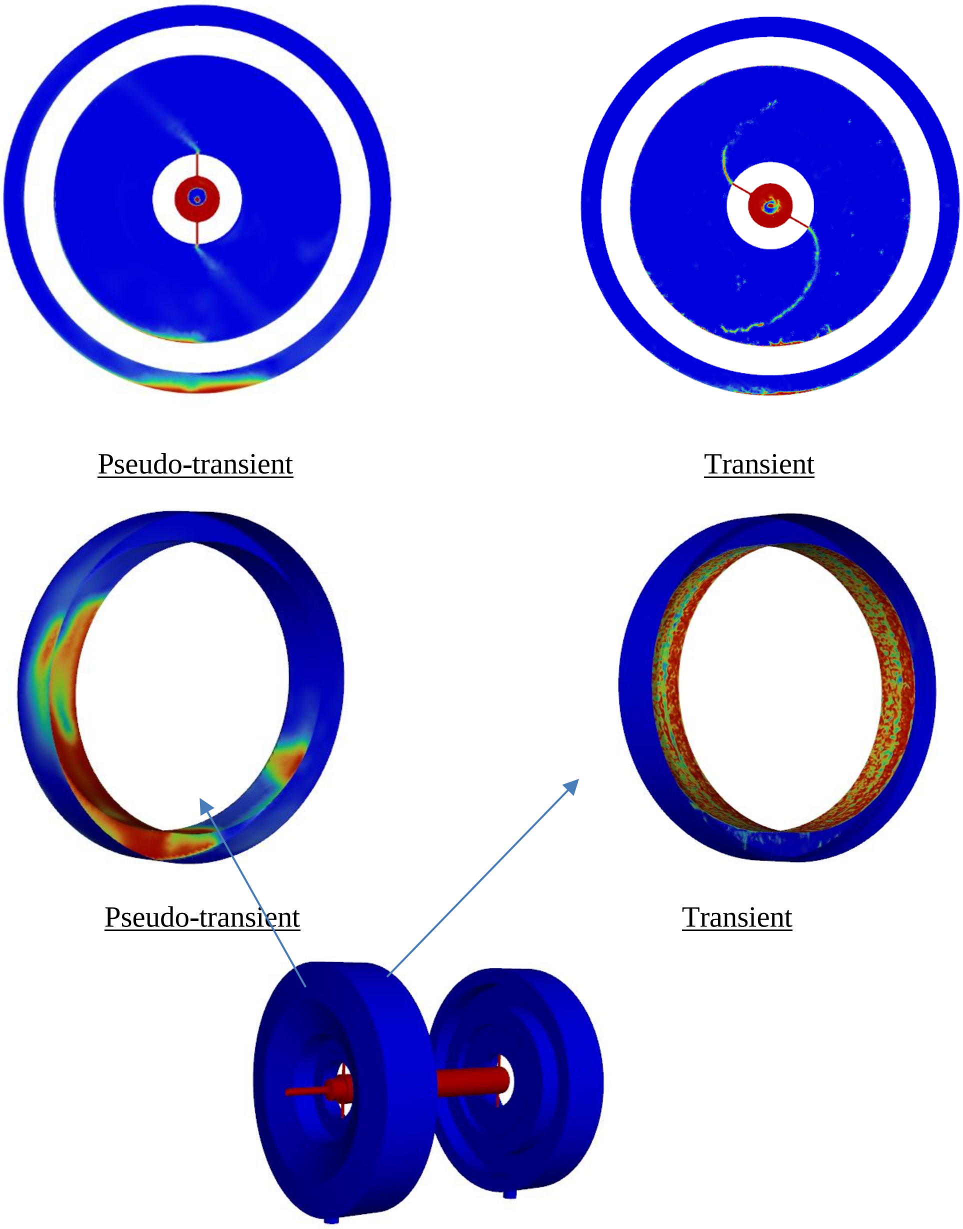

Fig. 41 (a) Pseudo transient phase contour of end space a (b) Transient phase contour of end space b (c) Pseudo transient phase contour of a side cell zone (d) Transient phase contour of b side cell zone

The contours of end-space region are compared between pseudo-transient and transient approach. It is observed that the oil wetting of end-space-a in pseudo-transient simulation using moving reference frame has most wetting area is in the gravity direction. Since, the shaft is not rotating in this case. Whereas the contour in transient result shows the uniformity of wetting throughout the winding domain. Due to sliding mesh motion of the shaft.

Solution Contours:

The contour images extracted from the transient simulation results are shown here.

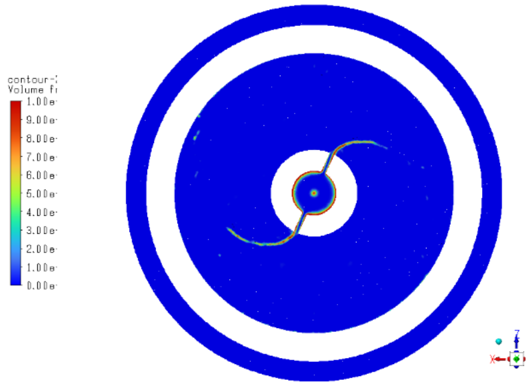

Fig. 42 Phase contour showing the oil trajectory of end space region

The contour Fig.36 shows the mid-plane of end-space region showing the oil trajectory coming out shaft nozzle and reaching winding area.

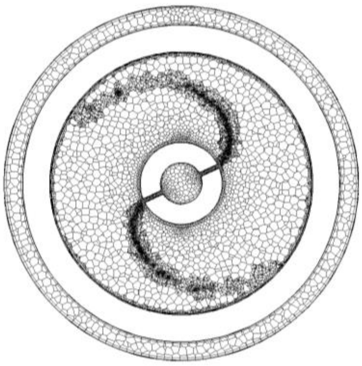

Fig. 43 Mesh contour of end-space region showing mesh adaption

The image Fig. 37 shows the mesh contour taken from the mid-plane of end-space region showing automatic mesh adaption technique. The oil region on the oil trajectory is automatically getting refined based on the area of interest.

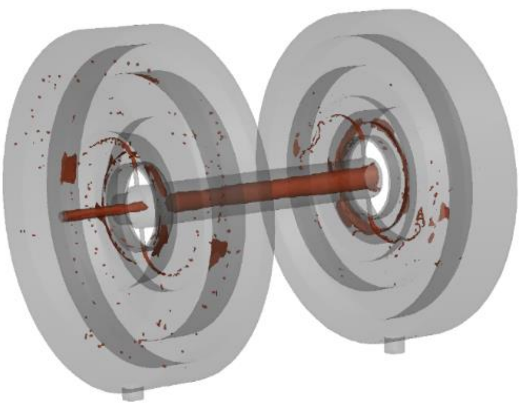

Fig. 44 Representation of oil wetting phenomenon shown in oil-filling contours of shaft with end windings

The contour Fig. 38 shows the shaft with end-winding region showing the scene of clipped surface with oil fraction more than 0.5, merged as a scene with iso-surface, wet wall, dry wall and body wall in an isometric view. Similarly, the contour Fig 39 shows the mid-section of shaft in a front view, showing the shaft filled with oil with nozzles spraying oil on the end windings.

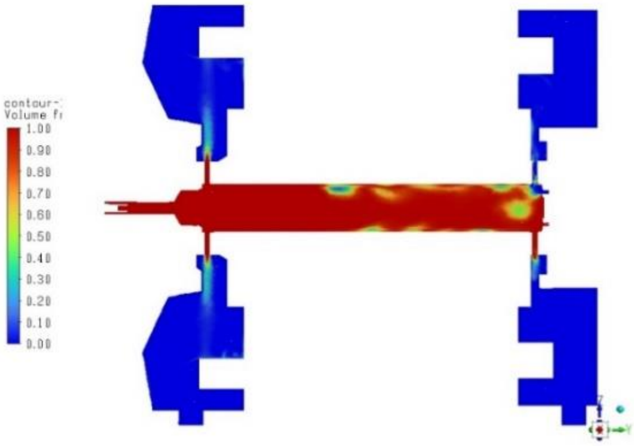

Fig. 45 Oil fraction contour of mid plane of shaft with end-windings

The contour Fig. 40 shows the scene of oil-filling contour having oil-circuit, rotor shaft, rotor laminations, and end-space regions captured at a flow time of 1.2 seconds. where the wetting stability has achieved. In this model the cell zone condition used for shaft is sliding mesh motion and for rotor lamination is MRF motion.

Fig. 46 Phase contour of complete fluid domain after wetting stability of transient run

The flow of oil in the rotor body and the windings can be observed. The splashing of oil after the stability of transient run can be observed from the contour. The image shows the oil-phase contour of the fluid-rotor volume, which constitutes of rotor laminations and the oil passage on it, for cooling the rotor and to avoid the magnets in getting demagnetized.

6.3 <u>Results of Mixed- time step coupling</u>

Once the wetting area gets stabilized on the windings, the flow equations are no further needed to be solved and only energy equation is required to be solved. A reference temperature is initially given to the heat generating source of the fluid domain, and their HTC & instantaneous temperature plots are computed from the fluid simulation. Then the heat flux value is given on the heat generating source of the solid windings and the HTC value computed from the fluid simulation are mapped to the adjacent solid walls, and their temperature values are plotted. This process is continued till the wall temperature gets stabilized.

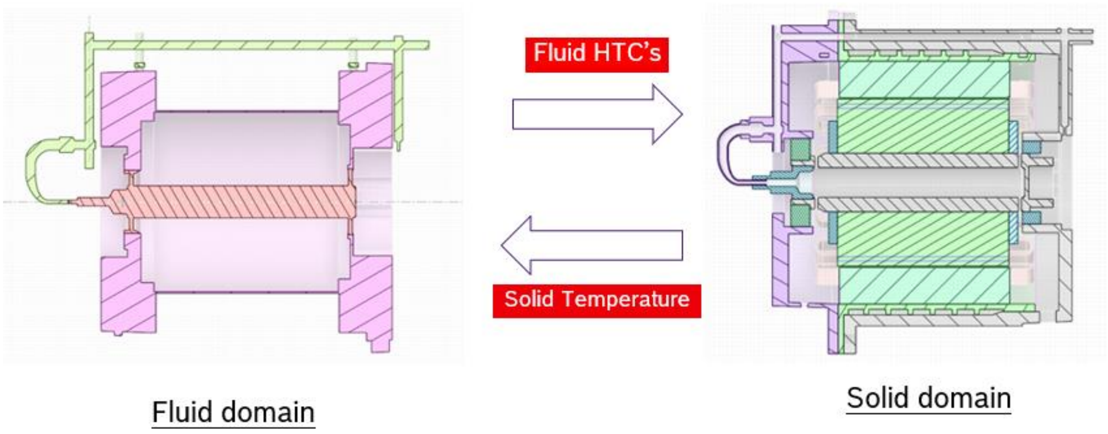

Fig. 47 Pictorial representation of the "mixed timescale coupling" approach used for studying the conjugate heat transfer.

Fluid Simulation			
Input Boundary conditions			
Parameters	**Specification**	**Value**	**Unit**
Average temperature	Winding a	180	°C
	Winding b	180	°C
	Rotor volume	110	°C
Output Results			
Average Heat Fux	Stator wall	46976	W/m^2
Net heat transfer rate	Fluid domain	10095	W

Table 6, The input Boundary condition and the output results of the fluid simulation results

The table 6 shows the initial reference temperature of windings and the extracted heat flux results. And the table 7 shows the mapped fluid simulation results to the solid model. The inlet temperature of the coolant, average temperature of the stator heat source, average heat flux and net heat transfer rate are given as input parameter to the solid simulation. And the area-weighted average temperature of both the end windings are computed. The deviations are checked in this iteration and this deviation are meant to be reduce in further iterations.

Solid Simulation			
Input Boundary conditions			
Parameters	**Specification**	**Value**	**Unit**
Average temperature	Coolant inlet	70	°C
Average temperature	Stator heat source	110	°C
Net heat transfer rate	Fluid domain	10095	W
Output Results			
Average temperature	Coolant outlet	97.6	°C
Average temperature	End windings a	156.48	°C
Average temperature	End windings b	163.67	°C
Average Heat Fux	Stator wall	46976	W/m^2

Table 7 The input Boundary condition and the output results of the solid simulation results

For stator cooling, the inlet coolant temperature is given as 70°C with the heat source temperature as 110°C. With this input parameter, the solid simulation gives the coolant output temperature as 97.6°C and the heat flux from the stator wall came out to be 46976 W/m^2. The contours of Coolant channel are shown below which shows the temperature distribution of stator housing having cooling channel designed.

For the area-weighted average temperature results of end windings are shown in the Table 7, this temperature values are to be computed with the initial reference temperature value. The temperature deviation for this iteration is 23.5°C for a-side end winding and 16.5°C for b-side end windings. This deviation gets reduce with further iteration. Based on this simulation results, the temperature contours can be plotted for multiple components and their higher temperature or hotspot zones can be captured.

Temperature contours of solid simulation

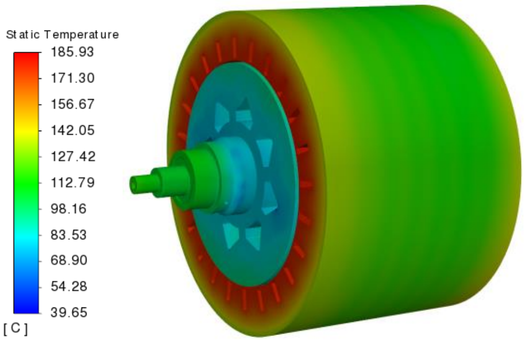

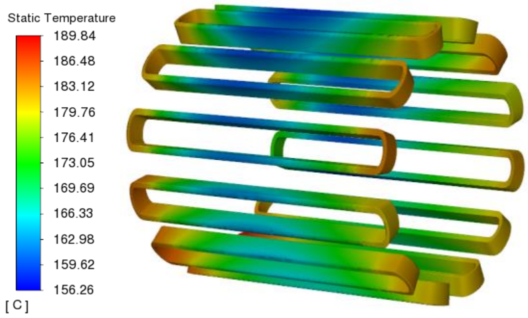

Rotor & Stator **Windings**

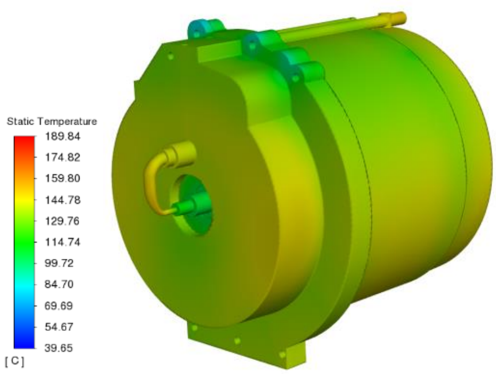

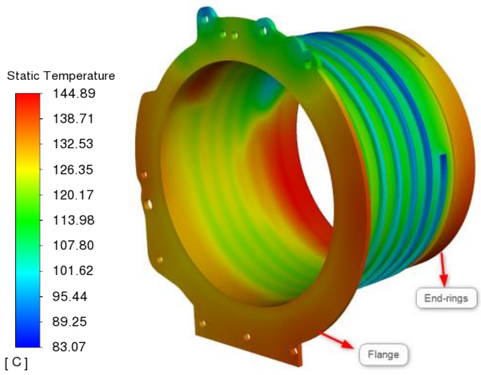

Outer housing **Cooling jacket**

Fig. 48 Temperature contour of (a) Rotor & stator (b) Windings (c) Outer housing (d) Cooling jacket

Observation:

- Among all the motor components, the maximum temperature is achieved on the stator end windings, i.e., up to 189°C.
- Majority of the heat gets removed using coolant, thus the end-windings shows relatively higher temperature than the main windings.
- The outer housing has an average static temperature of 110°C and does not reach the maximum temperature limit.
- The temperature of the cooling jacket is lower due to coolant flow. The end-ring zone and the flange are the hotspot zone having higher temperature, as it is close to the end windings region.
- Further iterations are to be done as a future scope for capturing exact hotspot regions among the motor components using mixed time scale coupling method.

Chapter: 7

Conclusions and Future Scope:

The primary purpose of this simulation study is to develop a numerical methodology for the oil cooling of Electric motors using Ansys Fluent simulation software. This study focusses on understanding the flow behavior of oil inside the rotor shaft and flow distribution through the radial nozzles fitted into it. This oil flow distribution within the shaft nozzles at different flow parameters has been studied and has been validated.

- It is found that the flow of oil in the front and rear side nozzle is in the ratio of 0.91-1.08.
- Further the transient simulation has been conducted for computing oil wetting area of the end-windings. The wetting percentage of the end windings are calculated as 27 % which gives 7% higher wetting area than that using pseudo transient approach.
- The temperature profile of the motor components is computed using mixed timescale coupling method. The amount of extracted heat and the temperature profiles are calculated, based on which the hotspot area of windings can be found.
- The computational time has been compared after using some new features of Ansys Fluent like Hybrid NITA and PUMA, and the computational time has been reduced drastically.

This study can further help in evaluating the thermal stresses and the fatigue life of the motor components. And the results can also help the design engineer to come up with better design of E-machine components. This methodology is to be implemented on actual motor geometry with hairpin-windings to compare the computational time required for simulation as a future study.

References

1. Srinivasan, Chiranth & Yang, Xiaofeng & Schlautman, Jeff & Wang, Deming & Gangaraj, Srihari. (2020). Conjugate Heat Transfer CFD Analysis of an Oil Cooled Automotive Electrical Motor. 10.4271/2020-01-0168.
2. Boglietti and A. Cavagnino, "Analysis of the Endwinding Cooling Effects in TEFC Induction Motors," in IEEE Transactions on Industry Applications, vol. 43, no. 5, pp. 1214-1222, Sept.-oct. 2007,
3. Y. Gai et al., "On the Measurement and Modeling of the Heat Transfer Coefficient of a Hollow-Shaft Rotary Cooling System for a Traction Motor," in IEEE Transactions on Industry Applications, vol. 54, no. 6, pp. 5978-5987, Nov.-Dec. 2018.
4. Boglietti and A. Cavagnino, "Analysis of the Endwinding Cooling Effects in TEFC Induction Motors," in IEEE Transactions on Industry Applications, vol. 43, no. 5, pp. 1214-1222, Sept.-oct. 2007.
5. Kea-Ho Lee, Hyun-Rok Cha, Young-Bae Kim, Development of an interior permanent magnet motor through rotor cooling for electric vehicles, Applied Thermal Engineering, Volume 95, 2016, Pages 348-356, ISSN 1359-4311.
6. J. Nonneman, B. van der Sijpe, I. T'Jollyn, S. Vanhee, J. Druant and M. de Paepe, "Evaluation of High Performance Rotor Cooling Techniques for Permanent Magnet Electric Motors," 2021 IEEE International Electric Machines & Drives Conference (IEMDC), Hartford, CT, USA, 2021, pp. 1-7.
7. B. Assaad, K. Mikati, T. V. Tran and E. Negre, "Experimental Study of Oil Cooled Induction Motor for Hybrid and Electric Vehicles," 2018 XIII International Conference on Electrical Machines (ICEM), Alexandroupoli, Greece, 2018, pp. 1195-1200.
8. P. -O. Gronwald and T. A. Kern, "Traction Motor Cooling Systems: A Literature Review and Comparative Study," in IEEE Transactions on Transportation Electrification, vol. 7, no. 4, pp. 2892-2913, Dec. 2021.
9. “Innovative Design of the Cooling Topologies for Electric Vehicle Motors” Published under licence by IOP Publishing Ltd ZHANG ZI-CHAO et al 2019 IOP Conf. Ser.: Mater. Sci. Eng. 533.
10. Xuehui Wang, Bo Li, Kuo Huang, Yuying Yan, Ian Stone, Sean Worrall, Experimental investigation on end winding thermal management with oil spray in electric vehicles, Case Studies in Thermal Engineering, Volume 35,2022,102082,ISSN 2214-157X,
11. Pin Chen, Nidhal Ben Hassine, Safouene Ouenzerfi, Souad Harmand, Experimental and numerical study of stator end-winding cooling with impinging oil jet, Applied Thermal Engineering, Volume 220,2023,119702, ISSN 1359-4311,
12. Grey relational based Taguchi analysis on heat transfer performances of direct oil spray cooling system for electric vehicle driving motor, Kunal Sandip Garud, Moo-Yeon Lee, International Journal of Heat and Mass Transfer, Volume 201, Part 2,2023,123596,ISSN 0017-9310
13. R. Sharma et al., “Efficient CFD Methodology for Optimal Design of Oil Cooled Electric Motor Shaft” Proceedings of the 7th World Congress on Momentum, Heat and Mass Transfer (MHMT'22) Lisbon, Portugal Virtual Conference – April 07 – 09, 2022 Paper No. ICMFHT 111
14. Conjugate Heat Transfer CFD Analysis of an Oil Cooled Automotive PMS Motor, Giovanni Cappelli
15. http://hevpdd.ca/wp-content/uploads/2020/05/Thermal-Management-of-PMSM-Using-LPTN-Model-by-Muhammad-Towhidi.pdf
16. https://www.researchgate.net/figure/Torque-and-power-requirements-of-drive-system-in-electric-vehicles-16_fig2_348153072
17. https://lutpub.lut.fi/bitstream/handle/10024/101756/Thesis_Mariia%20Polikarpova_A4.pdf?sequence=2
18. http://kth.diva-portal.org/smash/get/diva2:740752/FULLTEXT01.pdf
19. https://www.idealsimulations.com/resources/courant-number-cfd
20. https://www.extremetech.com/extreme/204804-new-low-cost-cerium-alloy-magnets-developed-for-motors-and-turbines
21. https://www.macheforum.com/site/threads/geek-out-on-the-engineering-behind-the-mach-e.148/
22. Sheela, A. and Atshaya, M., 2020. Design of permanent magnet synchronous motor for electric vehicle application using finite element analysis. International Journal of Scientific & Technology Research, 9

ORIGINALITY REPORT

14%	12%	8%	5%
SIMILARITY INDEX	INTERNET SOURCES	PUBLICATIONS	STUDENT PAPERS

PRIMARY SOURCES

1	tudr.thapar.edu:8080 Internet Source	1%
2	www.idealsimulations.com Internet Source	1%
3	Rajesh Kumar, Rajesh Kumar Shukla, Alok Kumar, Arvind Kumar. "A computational study on air entrapment and its effect on convective heat transfer during droplet impact on a substrate", International Journal of Thermal Sciences, 2020 Publication	1%
4	www.scribd.com Internet Source	1%
5	www.researchgate.net Internet Source	1%
6	Submitted to University of Sheffield Student Paper	1%
7	dokument.pub Internet Source	<1%